



Title	Role of marine nitrogen-fixing organisms in the formation of atmospheric reactive nitrogen
Author(s)	土橋, 司
Citation	北海道大学. 博士(環境科学) 甲第15259号
Issue Date	2023-03-23
DOI	10.14943/doctoral.k15259
Doc URL	<a href="http://hdl.handle.net/2115/89471">http://hdl.handle.net/2115/89471</a>
Type	theses (doctoral)
File Information	Dobashi_Tsukasa.pdf



[Instructions for use](#)

**Role of marine nitrogen-fixing organisms in the  
formation of atmospheric reactive nitrogen**

(大気反応性窒素の放出生成に対する  
海洋窒素固定生物の役割)

DISSERTATION

Dobashi Tsukasa  
16 February 2023

GRADUATE SCHOOL OF ENVIRONMENTAL SCIENCE  
HOKKAIDO UNIVERSITY



# Acknowledgements

This thesis is the result of the work for three years and a half at the Graduate School of Environmental Science and the Institute of Low Temperature Science, Hokkaido University. I worked with many people who helped me directly or indirectly during this time. I want to thank everyone for their expert advice, support, and encouragement throughout the work of this project.

I would particularly like to express my deepest gratitude and respect to my supervisor **Asst. Prof. Yuzo Miyazaki** for his guidance, discussion and advice. Through this research study, he kindly taught me how to approach and think about my search and attitude toward it. I would also like to give my special thanks to **Ms. Eri Tachibana** for the detailed instructions on experimental methods and precautions in chemical analyses and measurements. I am also grateful to the members of the Atmospheric Chemistry Group in the Institute of Low Temperature Science and the Course of Biogeochemistry in the Division of Earth System Science at the Graduate School of Environmental Science, Hokkaido University for their continuing encouragement and support.

I owe my deepest gratitude to the review committee members of the Graduate School of Environmental Science for their helpful advice during my pre- and final defenses. I acknowledge **Prof. Koji Suzuki**, who kindly taught me about the incubation experiment as well as many kind and helpful suggestions on my research. I also thank **Prof. Yoshito**

**Chikaraishi, Assoc. Prof. Yohei Yamashita, Prof. Jun Nishioka** for their valuable comments on this thesis.

I would express my gratitude to the coauthors of my paper on cruise KH-17-4, **Prof. Kazutaka Takahashi** (Graduate School of Agricultural and Life Sciences, The University of Tokyo), **Dr. Sachiko Horii** (Fisheries Resources Institute, Japan Fisheries Research and Education Agency), **Assoc. Prof. Fuminori Hashihama** (Department of Ocean Sciences, Tokyo University of Marine Science and Technology), **Dr. Saori Yasui-Tamura** (Department of Ocean Sciences, Tokyo University of Marine Science and Technology), **Assoc. Prof. Yoko Iwamoto** (Graduate School of Integrated Sciences for Life, Hiroshima University), **Dr. Shu-Kuan Wong** (National Institute of Polar Research), and **Prof. Koji Hamasaki** (Atmosphere and Ocean Research Institute, The University of Tokyo) for collecting aerosols in the atmosphere, providing the data of chlorophyll *a*, dissolved organic nitrogen,  $\text{NH}_4^+$ ,  $\text{NO}_3^-$ ,  $\text{NO}_2^-$ , primary production and nitrogen fixation rate in seawater during the KH-17-4 cruise. They also provided helpful comments on this work.

## Abstract

Marine atmospheric reactive nitrogen emitted from the sea surface is an important factor that affects air quality and climate over the ocean via influencing atmospheric photochemical field, particle formation, and cloud formation. Among atmospheric reactive nitrogen, water-soluble organic nitrogen (WSON) and ammonia/ammonium affect the particle formation, water-solubility, acidity, and light-absorbing properties of aerosol particles. First, size-segregated aerosol and surface seawater (SSW) samples were simultaneously collected over the subtropical North Pacific to investigate the origin of aerosol WSON in the marine atmosphere. The fine-mode WSON concentration at 200–240°E along 23°N defined as the eastern North Pacific (ENP) was significantly higher than that at 135–200°E, defined as the western North Pacific (WNP). Analysis of the stable carbon isotope ratio of water-soluble organic carbon (WSOC) ( $\delta^{13}\text{C}_{\text{WSOC}}$ ) together with backward trajectory indicated that most of the observed WSON in the fine particles in the ENP originated from the ocean surface. Positive relations were found among nitrogen fixation rate, dissolved organic nitrogen (DON) in SSW, and the WSON concentrations. The result suggests that reactive nitrogen (DON and ammonia), produced and exuded by nitrogen-fixing microorganisms in SSW, contributed to the formation of WSON aerosols.

To demonstrate the contribution of nitrogen-fixing microorganisms to the formation of atmospheric reactive nitrogen, including WSON, a laboratory incubation experiment was

conducted, using *Trichodesmium erythraeum* IMS101 (hereafter referred to as *Trichodesmium*), which is one of the most representative nitrogen-fixing microorganisms. During the incubation period of approximately two months, the growth and decline of the nitrogen-fixing microorganisms were observed. During the exponential phase, the DN and DOC concentrations in seawater increased with increasing the chlorophyll-*a* concentration, suggesting that DN and DOC were exuded from *Trichodesmium* during that phase. Throughout the experiment, ammonium and ammonia were the most abundant reactive nitrogen (avg. ~70%) in both particle and gas phases, followed by WSON (avg. ~20%). During the decline and death phases, the concentrations of atmospheric ammonia and gas-phase basic WSON significantly increased, suggesting the decomposition of DN and dead *Trichodesmium* cells and/or photochemical reactions in seawater, followed by the production of low-molecular-weight, more volatile, basic DN that was more easily transferred from seawater to the atmosphere.

These results demonstrated sea-to-air emissions of WSON and ammonium/ammonia associated with the growth and decline of *Trichodesmium* for the first time. The basic-gas reactive nitrogen components significantly released from seawater can affect the acidity of the atmosphere, and their reactions with acidic gas species can promote the particle formation. This in turn leads to an increase in the particle number concentration, which can further affect the number of cloud particles and thus impact on climate over the ocean.

# Table of contents

<b>Abstract .....</b>	<b>V</b>
<b>List of publications .....</b>	<b>X</b>
<b>Chapter 1. General Introduction .....</b>	<b>1</b>
1.1 Marine atmospheric aerosols and their impact on climate .....	1
1.2 Atmospheric water-soluble organic nitrogen (WSON).....	2
1.3 Marine atmospheric NH <sub>4</sub> <sup>+</sup> and NH <sub>3</sub> .....	4
1.4 Marine nitrogen-fixing organisms as a possible origin of atmospheric reactive nitrogen ..	5
1.5 Objectives of the study .....	6
References .....	7
<b>Chapter 2. Origin of Water-soluble Organic Nitrogen in Marine Atmospheric Aerosols in the Subtropical North Pacific .....</b>	<b>13</b>
2.1 Introduction .....	13
2.2 Experimental .....	14
2.2.1 Aerosol sampling.....	14
2.2.2 Surface seawater (SSW) sampling and chlorophyll <i>a</i> (Chl- <i>a</i> ) analysis.....	15
2.2.3 Chemical analysis of water-soluble aerosols and elemental carbon.....	16
2.2.4 Stable carbon isotopic characterization of water-soluble organic aerosols .....	17
2.2.5 Estimation of nitrogen-fixation rate .....	17
2.2.6 Determination of dissolved inorganic and organic nitrogen .....	18
2.3 Results and Discussion.....	19
2.3.1 Longitudinal distributions of WSON .....	19



2.3.2 Isotopic characterization of aerosol organic carbon and formation processes of WSON .....	21
2.3.3 Distributions of nitrogen fixation rate, dissolved organic nitrogen, and aerosol WSON .....	24
2.3.4 Discussion on nitrogen fixation as a possible source of WSON in marine aerosols..	27
2.4 Conclusions .....	31
References .....	33

**Chapter 3. Effects of Marine Nitrogen Fixation on Atmospheric Emissions of Reactive Nitrogen Revealed by a Laboratory Incubation Experiment .....** 49

3.1 Introduction .....	49
3.2 Experimental method .....	50
3.2.1 Incubation of <i>Trichodesmium</i> with artificial seawater and atmospheric sampling system.....	50
3.2.2 Incubation condition.....	51
3.2.3 Atmospheric sampling.....	52
3.2.4 Artificial seawater sampling.....	52
3.2.5 Chemical analysis of atmospheric samples .....	53
3.2.6 Measurements of chemical and biological parameters of artificial seawater .....	54
3.3 Results and discussion.....	54
3.3.1 Definition of growth phases of <i>Trichodesmium</i> .....	55
3.3.2 Temporal variation of DN and DOC in seawater .....	56
3.3.3 Temporal variation of atmospheric reactive nitrogen .....	57
3.3.4 Gas-particle phase partitioning and budget of reactive nitrogen species associated with the growth of <i>Trichodesmium</i> .....	59

3.3.5 Nitrogen-to-carbon ratios of the parameters in the atmospheric and seawater samples	60
3.3.6 Sea-to-air emission flux of reactive nitrogen	62
3.4 Conclusion	63
References	66
<b>Chapter 4. General Conclusions</b>	<b>85</b>

## **List of publications**

Dobashi, T., Miyazaki Y., Tachibana, E., Takahashi K., Horii, S., Hashihama, F., Yasui-Tamura, S., Iwamoto, Y., Wong, S. K., and Hamasaki, K.: Marine nitrogen fixation as a possible source of atmospheric water-soluble organic nitrogen aerosols in the subtropical North Pacific, *Biogeosciences*, 20, 439–449, <https://doi.org/10.5194/bg-20-439-2023>, 2023.

# **Chapter 1. General Introduction**

## **1.1 Marine atmospheric aerosols and their impact on climate**

The ocean covers about 70% of the Earth's surface and acts as a major source of atmospheric aerosols. Marine atmospheric aerosol is one of the key factors that control climate change, as they directly and indirectly (via the formation of cloud droplets) reflect and absorb sunlight, influencing the radiation budget [IPCC, 2021]. Cloud formation from marine atmospheric aerosols also affects amounts and processes of precipitation [Rosenfeld et al., 2019]. In the open ocean, marine atmospheric aerosols potentially impact the amount and reflectivity of low-level clouds [Garrett et al., 2004].

The most extensively studied marine atmospheric aerosols are sulfate and sea-salt particles, which are the main components of marine aerosols. Sulfate particles in the marine atmosphere are produced by the oxidation of dimethyl sulfide (DMS), which originates from the decomposition of dimethylsulphoniopropionate (DMSP) produced by marine organisms, particularly phytoplankton. Sulfate has been recognized as one of the most important components of marine aerosols as it can act as cloud condensation nuclei (CCN) to form cloud droplets [Weber et al., 1997].

On the other hand, studies in recent ~20 years have led to an improved understanding of marine organic aerosols (OAs) originating from the ocean surface. The production of marine OAs is associated with marine microbial activities, such as phytoplankton productivity, at the sea surface [O'Dowd et al., 2004]. Because organic matter in marine

aerosols can both promote and suppress cloud formation depending on their chemical components and particle mixing state [Miyazaki et al., 2020], it is important to understand the origin, formation process, amounts, and chemical/physical characteristics of OAs. There are two major formation processes of marine OAs: direct (primary) emissions as particles and secondary formation from gas-phase precursors such as volatile organic compounds (VOCs). Primary OA (POA) is emitted from the sea surface to the atmosphere as sea spray via bubble bursting and breaking waves. Previous studies reported that monosaccharides, amino acids, and proteins are present in marine POA and can serve as a biomarker for marine biological activity [Kuznetsova et al., 2005; Hawkins and Russell, 2010; Rastelli et al., 2017; Schiffer et al., 2018; Miyazaki et al., 2018; Zeppenfeld et al., 2021]. Marine secondary OA (SOA) is produced via the oxidation of volatile organic compounds (VOCs) emitted by phytoplankton and bacteria [Halsey et al., 2017; Davie-Martin et al., 2020; Fox et al., 2020; Moore et al., 2020; Croft et al., 2021; Zheng et al., 2021], as well as photochemical reactions in the sea surface microlayer (SML) [Bernard et al., 2016; Brüggemann et al., 2018]. However, there is still large uncertainty in our understanding of the amount, chemical composition, and formation processes associated with marine biota and marine atmospheric aerosols, particularly SOA.

## **1.2 Atmospheric water-soluble organic nitrogen (WSON)**

Atmospheric water-soluble organic nitrogen (WSON) has the potential to affect the

water solubility, light absorption, and acidity of aerosol particles, as well as the global biogeochemical cycling of nitrogen [Mohr et al., 2013; van Pinxteren et al., 2017; Facchini et al., 2008; Nehir and Kosak, 2018]. Some organic compounds with chemical structures containing nitrogen, such as imidazoles, can absorb light [Noziere et al. 2009], affecting the light-absorbing properties of aerosols and their ambient temperatures. In addition, some organic nitrogen in aerosols has both acid and base functional groups (e.g., nitro- and amino groups [Zhang et al., 2011]), which may affect the acidity of aerosol particles.

Most previous studies have traditionally focused on the atmospheric deposition of reactive nitrogen onto the ocean surface. This reactive nitrogen includes nitrate and ammonia, which are available for marine microorganisms. Duce et al. [2012] used a global chemical transport model to calculate the amount of atmospheric deposition of reactive nitrogen from terrestrial and marine origins into the ocean. They showed that atmospheric deposition of anthropogenic nitrogen resulted in up to 3% of annual oceanic new production, which emphasized the potential importance of the impact of nitrogen deposition on the ocean nitrogen cycle. In spite of many studies on inorganic nitrogen in terms of atmospheric deposition, the amount and origin of WSON in the marine atmosphere have little been understood.

Miyazaki et al. [2011] suggested a possible oceanic source of aerosol WSON for the first time based on the shipboard measurements in the western North Pacific. Altieri et al.

[2016] showed that WSON in marine aerosol was strongly correlated with surface ocean primary productivity and wind speed, suggesting a marine biogenic source of aerosol WSON in the western North Atlantic Ocean. Their study also indicated that the high concentrations of WSON aerosols were attributed to primary marine sources. These previous studies require our understanding of specific biogenic sources of WSON in the marine atmosphere associated with biota in seawater.

### **1.3 Marine atmospheric $\text{NH}_4^+$ and $\text{NH}_3$**

Gaseous ammonia ( $\text{NH}_3$ ) plays a key role in atmospheric chemical processes (and following deposition to the ocean) in the biogeochemical cycles.  $\text{NH}_3$  reacts rapidly with atmospherically-formed sulfuric and nitric acids to form fine particles existing as ammonium ( $\text{NH}_4^+$ ). Therefore,  $\text{NH}_3$  and  $\text{NH}_4^+$  are important factors that control the acidity of aerosol particles. Poulot et al. [2015] used global ocean biogeochemical models estimating the global oceanic emission of atmospheric  $\text{NH}_3$  to show that the ocean source dominates relative to terrestrial sources over the Equatorial Pacific. They suggested evidence for a missing source of atmospheric  $\text{NH}_3$  over the Equatorial Pacific that could be due to the photolysis of organic nitrogen (ON) at the ocean surface or in the atmosphere. Zhang and Anastasio [2003] reported the formation of  $\text{NH}_4^+$  from the photolysis of amino acids in the ocean. However, the oceanic sources of atmospheric  $\text{NH}_4^+$  and  $\text{NH}_3$  have not been well understood, as well as WSON.

## 1.4 Marine nitrogen-fixing organisms as a possible origin of atmospheric reactive nitrogen

Based on the background described in the previous sections, this thesis focuses on oceanic nitrogen-fixation processes as a possible new source of atmospheric reactive nitrogen over the ocean. Nitrogen fixation is a biological process that converts inert nitrogen ( $N_2$ ), which is metabolically useless to all but a few microorganisms, to reactive nitrogen ( $NH_4^+$ , dissolved ON (DON)). **Figure 1.1** shows the spatial distribution of nitrate concentration at the sea surface [World Ocean Atlas. 2018], while **Figure 1.2** shows the estimated nitrogen-fixation rates in the subtropical and tropical Pacific and western Atlantic [Gruber et al., 2016]. Over oligotrophic ocean areas, such as the subtropical and tropical Pacific, where the nitrate concentrations are deficient (**Figure 1.1**), nitrogen fixation rates are generally higher than in other regions (**Figure 1.2**).

A previous laboratory incubation experiment using nitrogen-fixing organisms showed that the production of DON was associated with the growth of nitrogen-fixing organisms [Berthelot et al., 2015]. In addition, Bonnet et al. [2016] estimated the amount of reactive nitrogen released by nitrogen-fixing organisms in seawater. *Trichodesmium* is a representative nitrogen-fixing organism, which is ubiquitously distributed in the subtropical ocean [Zehr and Capone. 2020]. Nitrogen fixation by *Trichodesmium* accounts for more than ~50 % of the total nitrogen fixation in the world ocean [Mahaffey



et al., 2005; Westberry et al., 2006]. However, the contribution of the nitrogen fixation process to the atmospheric emissions of reactive nitrogen has not been studied so far.

## **1.5 Objectives of the study**

The objective of this thesis is to elucidate the role of marine nitrogen-fixing microorganisms on the atmospheric emission and formation of reactive nitrogen (i.e., WSON and  $\text{NH}_3/\text{NH}_4^+$ ). So far, the influence of specific marine microorganisms on the sea-to-air emissions of reactive nitrogen has not been investigated. This thesis shows results from the shipboard measurements of aerosol WSON and biological/chemical parameters of surface seawater observed in the subtropical Pacific (Chapter 2). Then Chapter 3 presents the results of a laboratory incubation experiment using the representative nitrogen-fixing organism, *Trichodesmium erythraeum*, to observe resulting biological/chemical parameters in artificial seawater and discuss the atmospheric emissions of reactive nitrogen associated with the nitrogen-fixation process. General conclusions are presented in Chapter 4.

## References

- Alsante, A. N., Thornton, D. C. O., and Brooks, S. D.: Ocean Aerobiology, *Front. Microbiol.*, 12, 3143, <https://doi.org/10.3389/fmicb.2021.764178>, 2021.
- Altieri, K. E., Fawcett, S. E., Peters, A. J., Sigman, D. M., and Hastings, M. G.: Marine biogenic source of atmospheric organic nitrogen in the subtropical North Atlantic, *Proc. Natl. Acad. Sci. U.S.A.*, 113, 925–930, <https://doi.org/10.1073/pnas.1516847113>, 2016.
- Bernard, F., Ciuraru, R., Boréave, A., and George, C.: Photosensitized formation of secondary organic aerosols above the air/water interface. *Environ. Sci. Technol.* 50, 8678–8686. doi: 10.1021/acs.est.6b03520, 2016
- Brüggemann, M., Hayeck, N., and George, C.: Interfacial photochemistry at the ocean surface is a global source of organic vapors and aerosols. *Nat. Commun.* 9:2101. doi: 10.1038/s41467-018-04528-7, 2018.
- Croft, B., Martin, R. V., Moore, R. H., Ziemba, L. D., Crosbie, E. C., Liu, H., et al.: Factors controlling marine aerosol size distributions and their climate effects over the northwest Atlantic Ocean region. *Atmos. Chem. Phys.* 21, 1889–1916. doi: 10.5194/acp-21-1889-2021, 2021.
- Davie-Martin, C. L., Giovannoni, S. J., Behrenfeld, M. J., Penta, W. B., and Halsey, K. H.: seasonal and spatial variability in the biogenic production and consumption of volatile organic compounds (VOCs) by marine plankton in the North Atlantic Ocean. *Front. Mar. Sci.* 7:611870. doi: 10.3389/fmars.2020.611870, 2020.
- Duce, R.A., LaRoche, J., Altieri, K., Arrigo, K.R., Baker, A.R., Capone, D.G., Cornell, S., Dentener, F., Galloway, J., Ganeshram, R.S., Geider, R.J., Jickells, T., Kuypers, M.M., Langlois, R., Liss, P.S., Liu, S.M., Middelburg, J.J., Moore, C.M., Nickovic, S., Oschlies, A., Pedersen, T., Prospero, J., Schlitzer, R., Seitzinger, S., Sorensen, L.L., Uematsu, M., Ulloa, O., Voss, M., Ward, B., Zamora, L.: Impacts of atmospheric anthropogenic nitrogen on the open ocean, *Science*, 320, 893–897, 2008.
- Deutsch, C., Sarmiento, J.L., Sigman, D.M., Gruber, N., Dunne, J.P., Spatial coupling of nitrogen inputs and losses in the ocean. *Nature* 445, 163–167, 2007.
- Facchini, M.C., Decesari, S., Rinaldi, M., Carbone, C., Finessi, E., Mircea, M., Fuzzi, S.,

- Moretti, F., Tagliavini, E., Ceburnis, D., and O'Dowd, C.D.: Important Source of Marine Secondary Organic Aerosol from Biogenic Amines, *Environ. Sci. Technol.*, 42, 9116–9121, <https://doi.org/10.1021/es8018385>, 2008.
- Fox, J., Behrenfeld, M. J., Haëntjens, N., Chase, A., Kramer, S. J., Boss, E., et al.: Phytoplankton growth and productivity in the western North Atlantic: observations of regional variability from the NAAMES field campaigns. *Front. Mar. Sci.* 7:24. doi: 10.3389/fmars.2020.00024, 2020.
- Garrett, T. J., Zhao, C., Dong, X., Mace, G. C. and Hobbs, P. V.: Effects of Varying Aerosol Regimes on Low-Level Arctic Stratus, *Geophys. Res. Lett.*, 31, L17105, 2004.
- Garcia, H. E., K. Weathers, C. R. Paver, I. Smolyar, T. P. Boyer, R. A. Locarnini, M. M. Zweng, A. V. Mishonov, O. K. Baranova, D. Seidov, and J. R. Reagan, 2018. World Ocean Atlas 2018, Volume 4: Dissolved Inorganic Nutrients (phosphate, nitrate and nitrate+nitrite, silicate). A. Mishonov Technical Ed.; NOAA Atlas NESDIS 84, 35pp.
- Gruber, N.: Elusive marine nitrogen fixation. *Proc. Natl. Acad. Sci. U.S.A.* 113, 4246–4248. doi: 10.1073/pnas.1603646113, 2016.
- Halsey, K. H., Giovannoni, S. J., Graus, M., Zhao, Y., Landry, Z., Thrash, J. C., et al.: Biological cycling of volatile organic carbon by phytoplankton and bacterioplankton. *Limnol. Oceanogr.* 62, 2650–2661. doi: 10.1002/lno.10596, 2017.
- Hawkins, L. N., and Russell, L. M.: Polysaccharides, proteins, and phytoplankton fragments: four chemically distinct types of marine primary organic aerosol classified by single particle spectromicroscopy. *Adv. Meteorol.* 2010:612132. doi: 10.1155/2010/612132, 2010.
- IPCC, 2021: Climate Change 2021: The Physical Science Basis. Contribution of Working Group I to the Sixth Assessment Report of the Intergovernmental Panel on Climate Change [Masson-Delmotte, V., P. Zhai, A. Pirani, S.L. Connors, C. Péan, S. Berger, N. Caud, Y. Chen, L. Goldfarb, M.I. Gomis, M. Huang, K. Leitzell, E. Lonnoy, J.B.R. Matthews, T.K. Maycock, T. Waterfield, O. Yelekçi, R. Yu, and B. Zhou (eds.)]. Cambridge University Press, Cambridge, United Kingdom and New York, NY, USA, In press, doi:10.1017/9781009157896, 2021.
- Kuznetsova, M., Lee, C., and Aller, J.: Characterization of the proteinaceous matter in marine aerosols. *Mar. Chem.* 96, 359–377. doi: 10.1016/j.marchem.2005.03.007, 2005.

- Mahaffey, C., Michaels, and AF., Capone, DG.: The conundrum of marine Nitrogen fixation, *Am J Sci*,305:546–595, 2005.
- Maxut, A.; Nozière, B.; Fenet, B.; Mechakra, H. Formation Mechanisms and Yields of Small Imidazoles from Reactions of Glyoxal with NH<sub>4</sub><sup>+</sup> in Water at Neutral PH. *Phys. Chem. Chem. Phys.* 2015, 17 (31), 20416– 20424, DOI: 10.1039/C5CP03113C
- Miyazaki, Y., Kawamura, K., Jung, J., Furutani, H., and Uematsu, M.: Latitudinal distributions of organic nitrogen and organic carbon in marine aerosols over the western North Pacific, *Atmos. Chem. Phys.*, 11, 3037–3049, <https://doi.org/10.5194/acp-11-3037-2011>, 2011.
- Miyazaki, Y., Y. Yamashita, K. Kawana, E. Tachibana, S. Kagami, M. Mochida, K. Suzuki, and J. Nishioka.: Chemical transfer of dissolved organic matter from surface seawater to sea spray water-soluble organic aerosol in the marine atmosphere, *Scientific Reports*, 8, 14861, doi:10.1038/s41598-018-32864-7,2018.
- Miyazaki, Y., K. Suzuki, E. Tachibana, Y. Yamashita, A. Müller, K. Kawana, and J. Nishioka.: New index of organic mass enrichment in sea spray aerosols linked with senescent status in marine phytoplankton, *Scientific Reports*, 10, 17042, doi:10.1038/s41598-020-73718-5, 2020.
- Mohr C, Lopez-Hilfiker FD, Zotter P, Prevot ASH, Xu L, Ng NL, Herndon SC, Williams LR, Franklin JP, Zahniser MS, Worsnop DR, Knighton WB, Aiken AC, Gorkowski KJ, Dubey MK, Allan JD, and Thornton JA: Contribution of nitrated phenols to wood burning brown carbon light absorption in Detling, United Kingdom during winter time, *Environ. Sci. Technol*, 47, 6316–6324, 2013.
- Moore, E. R., Davie-Martin, C. L., Giovannoni, S. J., and Halsey, K. H.: Pelagibacter metabolism of diatom-derived volatile organic compounds imposes an energetic tax on photosynthetic carbon fixation. *Environ. Microbiol.* 22, 1720–1733. doi: 10.1111/1462-2920.14861, 2020.
- Nehir, M. and Koçak, M.: Atmospheric water-soluble organic nitrogen (WSON) in the eastern Mediterranean: origin and ramifications regarding marine productivity, *Atmos. Chem. Phys.*, 18, 3603–3618, <https://doi.org/10.5194/acp-18-3603-2018>, 2018.
- Nielsen CJ, D’Anna B, Dye C, Graus M, Karl M, et al.: Atmospheric chemistry of 2-aminoethanol (MEA). *Energy Procedia* 4:2245–52, 2011.

- Noziere, B., Dziedzic, P. and Cordova, A.: Products and Kinetics of LiquidPhase Reaction of Glyoxal Catalysed by Ammonium Ions (NH<sub>4</sub><sup>+</sup>), *J. Phys. Chem. A*, 113, 231-237, 2009.
- O'Dowd, C. D., Facchini, M. C., Cavalli, F., Ceburnis, D., Mircea, M., Decesari, S., Fuzzi, S., Yoon, Y. J., and Putaud, J.-P.: Biogenically driven organic contribution to marine aerosol, *Nature*, 431, 676–680, 2004.
- Rastelli, E., Corinaldesi, C., Dell'Anno, A., Lo Martire, M., Greco, S., Cristina Facchini, M., et al.: Transfer of labile organic matter and microbes from the ocean surface to the marine aerosol: an experimental approach. *Sci. Rep.* 7:11475. doi: 10.1038/s41598-017-10563-z, 2017.
- Rosenfeld, D., Zhu, Y. N., Wang, M. H., Zheng, Y. T., Goren, T., and Yu, S. C.: Aerosol-driven droplet concentrations dominate coverage and water of oceanic low-level clouds, *Science*, 363, eaav0566, <https://doi.org/10.1126/science.aav0566>, 2019.
- Schiffer, J. M., Luo, M., Dommer, A. C., Thoron, G., Pendergraft, M., Santander, M. V., et al.: Impacts of lipase enzyme on the surface properties of marine aerosols. *J. Phys. Chem. Lett.* 9, 3839–3849. doi: 10.1021/acs.jpcclett.8b01363, 2018.
- van Pinxteren, M., Barthel, S., Fomba, K. W., Müller, K., von Tümpling, W., and Herrmann, H.: The influence of environmental drivers on the enrichment of organic carbon in the sea surface microlayer and in submicron aerosol particles-Measurements from the Atlantic Ocean, *Elementa Science of the Anthropocene*, 5, 35, <https://doi.org/10.1525/elementa.225>, 2017.
- Weber, R. J.; Marti, J. J.; McMurry, P. H.; Eisele, F. L.; Tanner, D. J.; Jefferson, A. Measurements of new particle formation and ultrafine particle growth rates at a clean continental Site, *J. Geophys. Res.*, 102, 4375– 4385, doi: 10.1029/96JD03656, 1997.
- Westberry, TK., and Siegel, DA.: Spatial and temporal distribution of Trichodesmium blooms in the world's oceans, *Global Biogeochem Cycles*, 20:GB4016, doi: 10.1029/2005GB002673, 2006.
- Zhang, X., Lin, Y.-H., Surratt, J. D., Zotter, P., Prévôt, A. S. H. and Weber, R. J.: Light-Absorbing Soluble Organic Aerosol in Los Angeles and Atlanta: A Contrast in Secondary Organic Aerosol, *Geophys. Res. Lett.*, 38, L21810, 011, 2011.
- Zehr, J. P. and Capone, D. G.: Changing Perspectives in Marine Nitrogen Fixation,

Science, 368, eaay9514, doi: 10.1126/science.aay9514, 2020.

Zeppenfeld, S., Van Pinxteren, M., Van Pinxteren, D., Wex, H., Berdalet, E., Vaqué, D., et al.: Aerosol marine primary carbohydrates and atmospheric transformation in the Western Antarctic Peninsula. ACS Earth Space Chem. 5, 1032–1047. doi: 10.1021/acsearthspacechem.0c00351, 2021.

Zhang, Q., Anastasio, C.: Conversion of fogwater and aerosol organic nitrogen to ammonium, nitrate, and NO<sub>x</sub> during exposure to simulated sunlight and ozone. Environ. Sci. Technol. 37(16):3522–30, 2003.

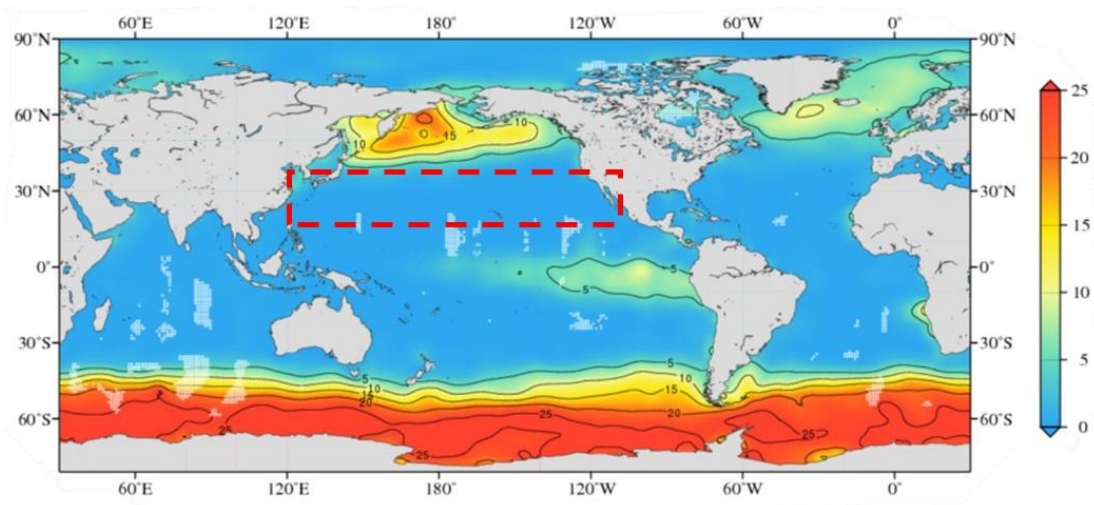


**Figure 1.1** Nitrate concentration at the sea surface ( $\mu\text{mol kg}^{-1}$ ) [World Ocean Atlas, 2018]. The original figure was slightly modified: the dashed rectangle in red indicates the oceanic nitrate depletion region of the tropical/subtropical North Pacific, where this thesis focuses on the nitrogen fixation process.

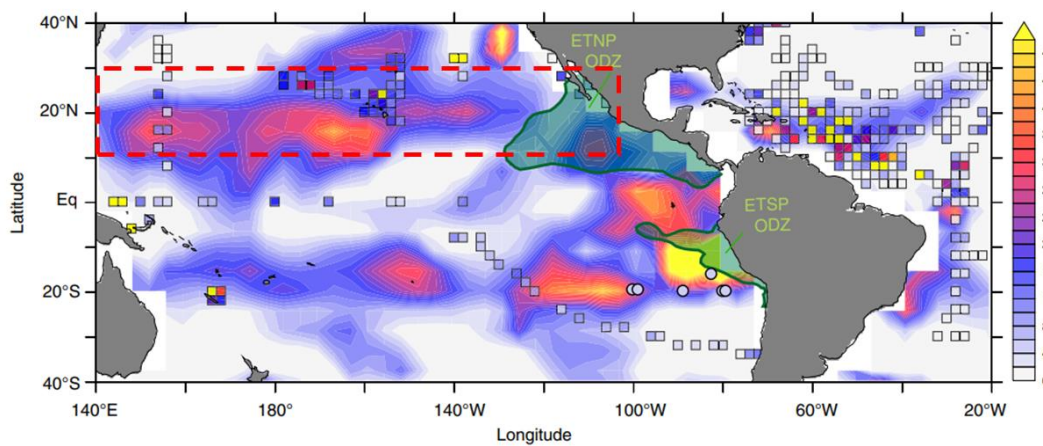


**Figure 1.2** Estimated (color contours) and observed (squares) values of nitrogen-fixation rate ( $\mu\text{mol m}^{-2} \text{d}^{-1}$ ) in the subtropical and tropical Pacific and western Atlantic [Gruber et al., 2016]. Estimated values were calculated from surface nutrients through an inverse modeling approach [Deutsch et al., 2007]. The original figure was slightly modified: the dashed rectangle in red indicates the oceanic region of the tropical/subtropical North Pacific with high nitrogen-fixing rates, focusing on the thesis.

# **Chapter 2. Origin of Water-soluble Organic Nitrogen in Marine Atmospheric Aerosols in the Subtropical North Pacific**

## **2.1 Introduction**

There is substantial uncertainty in our understanding of the linkage between the formation of aerosol WSON and marine microbial activity at the sea surface. Among the major groups of marine phytoplankton, cyanobacteria are the dominant primary producers in subtropical gyres [Rousseaux et al., 2012; Ottesen et al., 2014], which occupy one-third of Earth's surface. In particular, N<sub>2</sub>-fixing microorganisms, including cyanobacteria, are widely distributed in the subtropical North Pacific [Cheung et al., 2020; Zehr et al., 2020], which is a primarily oligotrophic area with a weak vertical supply of nitrate from below the euphotic layer [Shiozaki et al., 2017; Yamaguchi et al., 2021]. In this oceanic region, nitrogen fixation by marine microorganisms, such as *Trichodesmium*, a genus of filamentous cyanobacteria, is expected to be a possible source of reactive nitrogen in the atmosphere [Frischkorn et al., 2018]. However, the effects of N<sub>2</sub>-fixing microorganisms on the sea-to-air emissions of reactive nitrogen species, including WSON, have not yet been investigated.

This chapter aimed to elucidate the origin and formation process of WSON aerosols



in the oligotrophic subtropical ocean, particularly their linkage with N<sub>2</sub>-fixing microorganisms in surface seawater. WSON and other reactive nitrogen species were measured in size-segregated aerosols collected onboard a research vessel sailing over the subtropical North Pacific along the longitudinal transect in the summer of 2017. The discussion includes comparisons of the observed nitrogen aerosols with dissolved organic nitrogen (DON) concentrations and nitrogen fixation rates in SSW to investigate possible sources of WSON over the oceanic region.

## 2.2 Experimental

### 2.2.1 Aerosol sampling

Ambient aerosol sampling was conducted from 12 August to 5 October 2017 on board the research vessel *Hakuho Maru* [Hashihama et al., 2020; Yamaguchi et al., 2021]. Sampling was carried out during cruise KH-17-4 from Vancouver to Tokyo via Honolulu in the subtropical North Pacific (**Figure 2.1**). The aerosol samples were collected using a high-volume air sampler (HVAS; Model 120SL, Kimoto Electric, Osaka, Japan) located on the deck above the bridge of the ship. A cascade impactor (CI; Model TE-234, Tisch Environmental, Cleves, OH, USA) was attached to the HVAS to collect size-segregated particles at a flow rate of  $\sim 1130 \text{ L min}^{-1}$ , without temperature or humidity control. In the present study, we used analytical results obtained from the one bottom stage and four upper stages of the impactor, which collected particles with aerodynamic diameter ( $D_p$ ) <

0.95  $\mu\text{m}$  every 12 or 24 h and  $D_p > 0.95 \mu\text{m}$  every 96 h, respectively. Aerosol particles collected at the bottom and upper stages were referred to as fine and coarse particles, respectively. The atmospheric residence time of fine particles is typically  $\sim 1$  week, whereas that of coarse particles is generally much shorter (e.g.,  $\sim$ hours to days). To avoid possible contamination from ship exhaust during aerosol sampling, the sampling pump of the HVAS was shut off when the relative wind direction was out of  $\pm 60$  degrees to the bow and/or when the relative wind speed was low ( $< 5 \text{ m s}^{-1}$ ).

The aerosol samples were collected on quartz fiber filters (25 cm  $\times$  20 cm), which were precombusted at 450  $^{\circ}\text{C}$  for 6 h to remove any contaminants. Each collected filter was stored in a glass jar with a Teflon-lined screwed cap at  $-20^{\circ}\text{C}$  to limit chemical reactions on the filter and losses of volatile compounds. In this study, aerosol samples collected with a total air volume  $< 100 \text{ m}^3$  were not used. In total, 51 and 9 samples are presented for the fine and coarse particles, respectively. These numbers accounted for 88% and 82% of the total numbers of fine and coarse aerosol samples collected, respectively.

### **2.2.2 Surface seawater (SSW) sampling and chlorophyll *a* (Chl-*a*) analysis**

SSW samples were collected overboard at the depth of 0 m using an acid-cleaned bucket during each aerosol-sampling duration. The average temperature of SSW at each sampling point was  $26.1 \pm 2.1^{\circ}\text{C}$ . In total, analytical results of 12 SSW samples obtained

along 23°N were shown in the present study. The SSW samples for Chl-*a* analysis were filtered using 25-mm Whatman GF/F filters (GE Healthcare, Buckinghamshire, UK). Chl-*a* concentrations were further measured fluorometrically using 10-AU™ field and laboratory fluorometers (Turner Designs, Sunnyvale, CA) after extraction with N', N'-dimethylformamide [Suzuki and Ishimaru,1990].

### **2.2.3 Chemical analysis of water-soluble aerosols and elemental carbon**

To measure the concentrations of water-soluble organic carbon (WSOC) and water-soluble total nitrogen (WSTN) in the aerosol filter samples, a filter cut of 19.63 cm<sup>2</sup> was extracted with 15 mL of ultrapure water under ultrasonication and filtered using a disk filter (Millex-GV, 0.22 μm, Millipore, Billerica, MA, USA). The concentrations of WSOC and WSTN were determined using a total organic carbon (TOC) analyzer with a TN unit (Model TOC-L<sub>CHP</sub>+TNM-L, SHIMADZU). The sample was first injected into a combustion tube in the analyzer, which is filled with an oxidation catalyst (fiber platinum on quartz) and heated to 720°C to derive nitrogen monoxide under a constant flow of ultra-pure air. The nitrogen content was determined by measuring nitrogen monoxide with an ozone chemiluminescence detector [Miyazaki et al., 2011]. Additionally, another cut of the filter (7.07 cm<sup>2</sup>) was extracted with 10 mL of ultrapure water to measure the concentrations of Na<sup>+</sup>, NH<sub>4</sub><sup>+</sup>, NO<sub>3</sub><sup>-</sup>, NO<sub>2</sub><sup>-</sup>, and MSA. The same syringe filter type as described above was used, before the extract was injected into an ion chromatograph

(Model 761 compact IC; Metrohm). Here the WSON concentration was defined as the difference between the WSTN and inorganic nitrogen ( $\text{NH}_4^+$ ,  $\text{NO}_3^-$ ,  $\text{NO}_2^-$ ) concentrations. As an anthropogenic tracer, mass concentrations of elemental carbon (EC) were measured using a Sunset lab carbon analyzer. A filter punch of  $1.54 \text{ cm}^2$  was used for the analysis of EC.

#### **2.2.4 Stable carbon isotopic characterization of water-soluble organic aerosols**

To determine the  $\delta^{13}\text{C}$  of WSOC ( $\delta^{13}\text{C}_{\text{WSOC}}$ ) in the collected aerosols, a portion of the filter ( $9.08 \text{ cm}^2$ ) was extracted with 20 mL of ultrapure water. The extracted samples were then concentrated via rotary evaporation, and 40  $\mu\text{L}$  of each sample was transferred to be absorbed onto 15 mg of precombusted Chromosorb in a precleaned tin cup. The  $^{13}\text{C}_{\text{WSOC}}$  was then measured using an elemental analyzer (Flash EA 1112)/continuous flow carrier gas system (ConFlo)-isotope ratio mass spectrometer (Delta V, Thermo Finnigan) to determine the  $\delta^{13}\text{C}$  of WSOC ( $\delta^{13}\text{C}_{\text{WSOC}}$ ) [Miyazaki et al., 2012]. The  $^{13}\text{C}$  data were reported relative to an established reference of carbon Vienna PeeDee Belemnite (VPDB).

#### **2.2.5 Estimation of nitrogen-fixation rate**

Primary production and nitrogen fixation rates were determined using methods previously reported [Shiozaki et al., 2017], which followed Hama et al. [1983] and Mohr

et al. [2010], respectively. The SSW samples were collected using an acid-cleaned bucket. The SSW samples to estimate the initial  $^{15}\text{N}$  and  $^{13}\text{C}$  enrichment of POM were filtered immediately onto precombusted GF/F filters. For incubation  $^{13}\text{C}$ -labeled sodium bicarbonate (99 atom%  $^{13}\text{C}$ ; Cambridge Isotope Laboratories, Inc.) was added to each duplicate bottle at a final concentration of  $200\ \mu\text{mol L}^{-1}$ . The 110 mL of  $^{15}\text{N}_2$ -enriched SSW, in which 1.1 ml of  $^{15}\text{N}_2$  gas (>99 atom%  $^{15}\text{N}$ , Shoko Science) was dissolved using a Sterapore membrane unit (20M1500A: Mitsubishi Rayon Co., Ltd.), was added to each bottle. The samples were then incubated for 24 h using an on-deck incubator with surface SSW running continuously. The incubation was terminated by gentle vacuum filtration of the SSW samples through precombusted GF/F filters. The filters were then frozen at  $-20^\circ\text{C}$  until the post-measurement on the ground. The filter samples were dried at  $50^\circ\text{C}$  in an oven and were exposed to hydrogen chloride (HCl) fumes for 2 h to remove inorganic carbon, followed by being dried at  $50^\circ\text{C}$  again. The N and C contents and their stable isotope ratios were then determined using a DELTA V advantage mass spectrometer (Thermo Electron, USA) connected to an elemental analyzer. nitrogen fixation activity was regarded to be significant when the atom% of  $^{15}\text{N}$  for each incubated bottle was higher than that for the initial sample by 0.00146 atom% [Montoya et al., 1996]. Primary production and nitrogen fixation rates were determined twice at each sampling station.

### **2.2.6 Determination of dissolved inorganic and organic nitrogen**

Surface seawater samples for the determination of dissolved inorganic and organic nitrogen were collected at 10-m depth using a conductivity–temperature–depth (CTD) system (Sea-Bird Electronics) equipped with acid-cleaned Niskin-X bottles (General Oceanics) [Hashihama et al., 2020]. Total dissolved nitrogen (TDN) was measured by a persulfate oxidation method with a gas-segmented continuous flow analyzer [Yasui-Tamura et al., 2020]. TDN sample was converted to  $\text{NO}_3^-$  by oxidation and analyzed by colorimetric method. Concentrations of  $\text{NH}_4^+$  and  $\text{NO}_3^- + \text{NO}_2^-$  in seawater were determined by using sensitive liquid waveguide spectrophotometry [Hashihama et al., 2009; Hashihama et al., 2015]. DON concentration was determined as the difference between the TDN and dissolved inorganic nitrogen ( $\text{DIN} = \text{NH}_4^+ + \text{NO}_3^- + \text{NO}_2^-$ ) concentrations in surface seawater.

## 2.3 Results and Discussion

### 2.3.1 Longitudinal distributions of WSON

**Figures 2.2a** and **2.2b** show the longitudinal distribution of the concentrations of WSON in fine particles ( $\text{WSON}_F$ ) with particle diameter ( $D_P$ )  $< 0.95 \mu\text{m}$  and in coarse particles ( $\text{WSON}_C$ ) with  $D_P > 0.95 \mu\text{m}$  from samples collected at  $23^\circ\text{N}$  in the subtropical North Pacific (**Figure 2.1**). The average concentrations of  $\text{WSON}_F$  and  $\text{WSON}_C$  were  $6.1 \pm 6.2 \text{ ngN m}^{-3}$  and  $22 \pm 21 \text{ ngN m}^{-3}$ , respectively, during the cruise measurement. The sum of these values is within range of the WSON concentrations in total suspended

particles (TSP) collected over the western North Pacific [3.0–35 ngN m<sup>-3</sup>; Duce et al., 2008]. Here, along the cruise track at 23°N, the oceanic region at 200–240°E is defined as the eastern North Pacific (ENP), whereas the region at 135–200°E is defined as the western North Pacific (WNP). This classification corresponds to the two legs of the cruise: the first leg was from Vancouver to Honolulu, whereas the second one was from Honolulu to Tokyo. Concentrations of WSON in both the fine and coarse particles showed a distinct longitudinal gradient, with substantially higher concentrations in ENP. The average concentrations of WSON<sub>F</sub> and WSON<sub>C</sub> in ENP were approximately 3–6 times as large as those in the WNP (**Table 2.1**).

The longitudinal distributions of the mass concentrations of inorganic nitrogen (NH<sub>4</sub><sup>+</sup>, NO<sub>3</sub><sup>-</sup>, and NO<sub>2</sub><sup>-</sup>) generally showed similar patterns to those of WSON (**Figure 2.3**). The sum of the mass concentrations of the inorganic nitrogen in ENP was approximately twice as large as those in WNP. Overall, NH<sub>4</sub><sup>+</sup>-N was the dominant component of water-soluble total nitrogen (WSTN) (~78%) in the fine-mode aerosols, followed by WSON (16%) (**Figure 2.2c**). In contrast, NO<sub>3</sub><sup>-</sup>-N was the most abundant WSTN component of the coarse-mode aerosols, which accounted for 83% of the WSTN mass on average. Notably, the mass fraction of WSON in ENP was significant, accounting for up to ~50% (average: 19±15%) and ~11% of the WSTN in the fine- and coarse-particle masses, respectively (**Figures 2.2c and 2.2d**). This result indicates the importance of the abundance of WSON, particularly in the fine particles in ENP.

**Figure 2.2e** presents the concentrations of Chl-*a* in surface seawater (SSW) samples obtained during the cruise, as well as the average concentrations of Chl-*a* during August–September 2017 derived from the MODIS-Aqua ocean color data ([https://neo.sci.gsfc.nasa.gov/view.php?datasetId=MY1DMM\\_CHLORA&year=2017](https://neo.sci.gsfc.nasa.gov/view.php?datasetId=MY1DMM_CHLORA&year=2017)). The two different measurements of Chl-*a* generally showed similar longitudinal distributions, which resemble the longitudinal trend of the WSON concentrations. Moreover, 5-day back trajectories, calculated by HYSPLIT ([https://www.ready.noaa.gov/HYSPLIT\\_traj.php](https://www.ready.noaa.gov/HYSPLIT_traj.php)), showed that the sampled air masses were transported primarily over the oceanic regions in the Pacific (**Figure 2.1**). These results suggest that most of the observed aerosols were transported within the marine boundary layer with less influence from terrestrial sources prior to sampling. This is supported by the concentrations of nss-Ca<sup>2+</sup> and nss-K<sup>+</sup> as well as nss-SO<sub>4</sub><sup>2-</sup>/methanesulfonic acid (MSA) ratios which did not show significant differences between WNP and ENP (**Table 2.1**). Although the trajectory suggested that the observed air masses were influenced by other oceanic regions, they were diluted during the transported and were likely more influenced by the sampling areas nearby. The overall results suggested that the observed aerosols, particularly those in ENP, were largely influenced by marine sources associated with phytoplankton.

### **2.3.2 Isotopic characterization of aerosol organic carbon and formation processes of WSON**



Previously, a method using stable carbon isotope ratios ( $\delta^{13}\text{C}$ ) of aerosol organic carbon was successfully used to determine the contributions of marine and terrestrial sources to organic aerosols in the marine atmosphere [Cachier et al., 1986; Miyazaki et al., 2016]. The  $\delta^{13}\text{C}$  of water-soluble organic carbon (WSOC;  $\delta^{13}\text{C}_{\text{WSOC}}$ ) as a function of the  $\text{WSO}_{\text{N}_F}$  concentrations is shown in **Figure 2.4**. The  $\delta^{13}\text{C}_{\text{WSOC}}$  value was only available for  $\text{WSO}_{\text{C}_F}$  in this study. The average  $\delta^{13}\text{C}_{\text{WSOC}}$  observed in this study was  $-22.8 \pm 1.7\text{‰}$ , with 71% of the data (12 out of 17 data points) in the range of typical marine origin [between  $-24\text{‰}$  and  $-18\text{‰}$ ; Miyazaki et al., 2016], while that of terrestrial origin is between  $-27\text{‰}$  and  $-25\text{‰}$  [Cachier et al., 1986; Dasari et al., 2019]. This isotopic characterization supports that most of the organic carbon fractions of the observed aerosols were of marine origin.

To elucidate the possible formation processes of the observed WSON, we used several tracers of marine origins. **Figures 2.5a** and **2.5b** show scatter plots between WSON and  $\text{Na}^+$  concentrations. The concentrations of  $\text{Na}^+$ , used as a tracer of marine primary emissions, did not show any significant positive correlations with those of  $\text{WSO}_{\text{N}_F}$  ( $R^2 = 0.04$ ) or  $\text{WSO}_{\text{N}_C}$  ( $R^2 = 0.03$ ) in the study area. Specifically, the  $R^2$  value between  $\text{WSO}_{\text{N}_F}$  and  $\text{Na}^+_F$  was 0.003 in ENP, while  $\text{WSO}_{\text{N}_F}$  and  $\text{Na}^+_F$  concentrations even showed a negative correlation ( $R^2 = 0.49$ ) in WNP (**Figure 2.5a**). The correlation cannot be statistically discussed for the coarse mode separately in ENP and WNP due to the limited number of data points. Nevertheless, the WSON concentration was higher in the ENP

than in the WNP for the same  $\text{Na}^+$  concentration level in the coarse particles (**Figure 2.5b**), suggesting that WSON was more abundant relative to  $\text{Na}^+$  in coarse particles in ENP. Moreover, concentrations of glucose, a molecular tracer of marine primary aerosols [Miyazaki et al., 2018], were below the lower detection limit for most of the samples during the cruise. These results suggest insignificant contributions of direct emissions from the sea surface to the observed WSON.

The above results also imply that secondary formation was likely the dominant process underlying the formation of WSON observed in this study. The process includes accommodation of secondary WSON onto sea salt particles. **Figures 2.5c** and **2.5d** present scatter plots between WSON and MSA concentrations in each particle size category. MSA has been widely used as a tracer of marine SOA because it is an oxidation product of dimethyl sulfide (DMS). MSA is either produced by gas-phase MSA directly scavenged by aerosols or rapidly produced in the aqueous phase from scavenged dimethylsulfoxide (DMSO) and methanesulfinic acid (MSIA) [Zhu et al., 2006]. The concentrations of WSON did not show any significant correlations with those of MSA in each size range regardless of the oceanic region. The insignificant correlation suggests that the origin of the observed WSON aerosols differed from that of DMS or that the formation pathways of WSON were different from the oxidation processes of DMS. It is also possible that dependence of temperature and/or OH levels in the subtropics on the relative yields of MSA to sulfate in the oxidation of DMS [e.g., Mungall et al., 2018]

might also partly affect the insignificant correlations between WSON and MSA. In fact, no relations were found between sulfate, known as an oxidation product of DMS, and WSON concentrations ( $R^2 < 0.02$ ) in fine particles (data not shown). On the other hand, sulfate and WSON concentrations in coarse particles showed some positive relationships, although the number of data is limited. This may reflect overlapping processes of biogenic sulfate and WSON on a longer timescale (i.e., several days of sampling of coarse particles) even though the exact origins are different.

### **2.3.3 Distributions of nitrogen fixation rate, dissolved organic nitrogen, and aerosol WSON**

To further explore the origin and possible formation process of the observed WSON aerosols associated with phytoplankton, we focused on nitrogen fixation in SSW as a possible source of atmospheric reactive nitrogen. Nitrogen fixation is the biological conversion of  $N_2$  to  $NH_4^+$  or dissolved ON (DON), which represents the main external source of bioavailable nitrogen in marine environments. A significant fraction of fixed  $N_2$  can be directly released by  $N_2$ -fixing microorganisms as dissolved inorganic nitrogen ( $NH_4^+$ ,  $NO_3^-$ , and  $NO_2^-$ ) and DON in the ocean. Data obtained from Station ALOHA in the subtropical North Pacific have shown enrichment of nitrogen pools (i.e.,  $NH_4^+$ ,  $NO_3^-$ , DON) within *Trichodesmium* blooms [Karl et al., 1992; Letelier and Karl, 1994]. It has been shown that majority of the recently fixed  $N_2$  is released directly as DON during the growth of *Trichodesmium*, primarily as dissolved free amino acids [Capone et al., 1994;

Glibert and Bronk, 1994]. Luo et al. [2014] estimated that, on average, spatially integrated nitrogen fixation over the Pacific accounted for ~50% of that in the global ocean, pointing to the importance of the Pacific in terms of this process.

In the subtropical North Pacific, previously measured nitrogen isotope ratios ( $\delta^{15}\text{N}$ ) in particulate organic matter (POM) from seawater suggested that POM was significantly affected by nitrogen supplied from  $\text{N}_2$ -fixing microorganisms [Horii et al., 2018]. Indeed, in the current study, the average  $\delta^{15}\text{N}$  of POM in the SSW samples was  $-0.3 \pm 1.0$  ‰ (data not shown), which is within the range of  $\delta^{15}\text{N}$  values of diazotrophic cyanobacteria typically ranging from  $-2$  ‰ to  $0$  ‰ [Horii et al., 2018]. This indicates that the organic matter in SSW collected in the study region is derived from nitrogen supplied by  $\text{N}_2$ -fixing microorganisms such as cyanobacteria.

**Figure 2.6** shows the latitudinal distributions of the nitrogen fixation rate and concentrations of DON and TDN in the SSW samples compared with those of aerosol WSON concentrations in each size category. The average nitrogen fixation rate in the SSW samples collected in ENP was  $38.6 \pm 13.3$   $\text{ngN L}^{-1} \text{d}^{-1}$ , which was significantly higher than that in the WNP ( $11.5 \pm 10.6$   $\text{ngN L}^{-1} \text{d}^{-1}$ ). Phosphate concentrations in SSW showed similar longitudinal gradient, which is likely due to the P demand of microorganisms in this oceanic region [Hashihama et al., 2020]. The longitudinal gradient of nitrogen fixation rate depends on the distribution of phosphate, whose concentration was reported to be higher in the ENP than in the WNP. The observed range of the nitrogen

fixation rate in SSW is similar to those reported for the same oceanic region in previous studies [Montoya et al., 2004; Bonnet et al., 2009; Yamaguchi et al., 2019]. Moreover, the longitudinal gradient of the nitrogen fixation rate is similar to that along 23°N in the tropical Pacific, as shown by previous field measurements and model simulations [Luo et al., 2014; Dutheil et al., 2018; Wang et al., 2019; Shiozaki et al., 2018; Hashihama et al., 2020]. The higher nitrogen fixation rate in ENP compared to that in WNP could be attributed to the greater abundance of N<sub>2</sub>-fixing microorganisms such as *Trichodesmium* and a symbiotic unicellular cyanobacterium (UCYN-A) measured by quantitative polymerase chain reaction (qPCR) of *nifH*. In particular, the number of the *nifH* copy of UCYN-A in ENP was three orders of magnitude larger than that in WNP (data not shown).

The longitudinal distributions of DON clearly showed that DON concentrations in SSW of ENP ( $4.77 \pm 0.53 \mu\text{M}$ ) were larger than those of WNP ( $4.03 \pm 0.47 \mu\text{M}$ ) (**Figure 2.6c**). Furthermore, nitrogen fixation rate and DON concentrations in SSW showed a positive correlation with R<sup>2</sup> of 0.63, where DON concentration accounted for >98% of TDN concentration, which showed the dominance of DON in TDN during the cruise. These results suggest that the majority of DON in SSW were released in association with the recently fixed N<sub>2</sub> during the growth of N<sub>2</sub>-fixing microorganisms. It is noted that the nitrogen fixation rate was calculated for particulate nitrogen in this study, whereas Konno et al. [2010] suggested that nitrogen fixation rate of the filtrate fraction (i.e., similar to DON) accounted for on average 50% of the total nitrogen fixation rates in the western

North Pacific. That study points to possible underestimation of total nitrogen fixation rate discussed in this study.

The WSON concentrations in both fine and coarse particles showed positive correlations with the nitrogen fixation rates in the SSW samples (**Figures 2.6** and **2.7**), with  $R^2$  values of 0.27 ( $p < 0.05$ ) and 0.60 ( $p < 0.05$ ) in the fine and coarse modes, respectively. Additionally, concentrations of  $WSON_{F+C}$  and DON were positively correlated ( $R^2 = 0.36$ ,  $p < 0.05$ ). Meanwhile, the  $R^2$  values for the WSON concentrations and primary productivity in SSW were 0.08 ( $p = 0.24$ ) and 0.58 ( $p < 0.05$ ) in the fine and coarse modes, respectively (**Figures 2.8** and **2.9**), which were lower than those for WSON and nitrogen fixation rate. The positive relation between the WSON mass concentrations and nitrogen fixation rate together with the  $\delta^{15}N$  value of POM in SSW suggests that reactive nitrogen produced by  $N_2$ -fixing microorganisms in SSW significantly contributed to the formation of WSON aerosols.

#### **2.3.4 Discussion on nitrogen fixation as a possible source of WSON in marine aerosols**

Previous laboratory experiments also showed that DON and  $NH_4^+$  are released in seawater through nitrogen fixation by microorganisms known as diazotrophs [Wannicke et al., 2009; Berthelot et al., 2015]. Here, we discuss mass-based N:C ratios in seawater and atmospheric aerosols. The average WSTN:WSOC ratio in all the size ranges of the observed aerosols was  $1.70 \pm 0.94$ , while those in ENP and WNP were  $1.61 \pm 0.99$  and

1.87±0.82, respectively. It is noted that there may be bias in the WSTN:WSOC ratios, particularly in WNP, because the WSOC concentrations were below the detection limit in many samples. Yvon-Durocher et al. [2015] reported that the N:C ratios of marine algal assemblages over the subtropical Pacific ranged between 0.10 and 0.13, while Wannicke et al. [2009] obtained N:C ratios of *Trichodesmium* (0.21±0.02) through a laboratory experiment. Furthermore, Berthelot et al. [2015] reported that the ratio of dissolved nitrogen (DN) to DOC released during nitrogen fixation was 0.07±0.48. The currently observed WSTN:WSOC ratio in the aerosols was much higher than the N:C ratios of microbes and the DN:DOC ratios in seawater affected by nitrogen fixation. The higher WSTN:WSOC ratios in aerosols relative to the typical DN:DOC ratios in seawater suggest that nitrogen-containing aerosols are preferentially produced relative to organic carbon in the atmosphere.

It is possible to argue that anthropogenic sources might contribute to the observed WSTN, including WSON and  $\text{NH}_4^+$ , as well as WSTN:WSOC ratios in aerosols shown above. Concentrations of EC as an anthropogenic tracer were below the lower detection limit ( $\sim 0.1 \mu\text{gC m}^{-3}$ ) in all the aerosol samples, where they did not show any statistically significant differences between WNP and ENP (**Figure 2.6**). This result suggests that the effects of anthropogenic sources on the observed aerosols in ENP were likely small. This is consistent with the stable carbon isotope analysis, which suggested that most of the observed aerosols were of marine origin rather than terrestrial sources, including

anthropogenic origin. Although measurement data of gas species were not available in this study, it is unlikely that only gas-phase precursors were of anthropogenic origin, explaining the secondary formation of WSON, although most of the observed aerosols originated from the ocean surface.

Previous studies showed that oceanic regions at low latitudes, including the subtropics, act as a source of  $\text{NH}_3$  [the net flux of  $\text{NH}_3$  is out of the ocean to the atmosphere; Jickells et al., 2003; Johnson et al., 2008]. Paulot et al. [2015] used two global ocean biogeochemical models to show evidence for a missing source of atmospheric ammonia ( $\text{NH}_3$  and  $\text{NH}_4^+$ ) over the equatorial Pacific that was attributable to photolysis of marine ON at the ocean surface or in the atmosphere. In fact, DON was the dominant component of TDN (>98%) in surface seawater, the longitudinal distribution of which was similar to that of WSON in our study (**Figure 2.6**). Furthermore, the observed  $\text{NH}_4^+$  concentration levels in our study (ave. 40-50  $\text{ng m}^{-3}$ ) agree well with those predicted by Paulot et al. [2015] in the same oceanic region. Indeed,  $\text{NH}_4^+$  was the dominant component of the aerosol reactive nitrogen in the fine particles (**Figure 2.2c**) in this study, whereas the correlations between  $\text{NH}_4^+$  concentrations and nitrogen fixation rates were insignificant ( $R^2 = 0.06$ ). This insignificant correlation is partially attributable to the phase partitioning of ammonia into the gas phase in the subtropical region. A possible source of  $\text{NO}_3^-$  is not necessarily anthropogenic in the equatorial Pacific, while the contribution of an oceanic source in the open ocean cannot be ruled out. Several recent field studies suggested



oceanic sources of aerosol  $\text{NO}_3^-$  in the eastern equatorial Pacific with evidence of extremely low values of  $\delta^{15}\text{N}$  of  $\text{NO}_3^-$  [e.g., lower than  $-5\%$ ; Kamezaki et al., 2019; Carter et al. 2021]. In this oceanic region, alkyl nitrates are suggested to contribute to nitrate production, where relatively high concentrations of alkyl nitrates have been observed over the equatorial Pacific. The low concentrations of EC and stable carbon isotope ratios in aerosols, together with the higher concentrations of DON in ENP, partly supported the oceanic source of aerosol  $\text{NO}_3^-$  in this oceanic region, although  $\delta^{15}\text{N}$  of  $\text{NO}_3^-$  was not available in this study. To summarize, relatively high concentrations of inorganic nitrogen as well as WSON in ENP relative to WNP were also partly attributable to more active nitrogen fixation in ENP.

The secondary formation processes of WSON include emissions of gas-phase ON from the ocean and/or marine VOCs reacting with  $\text{NH}_3$  [Paulot et al., 2015; Altieri et al., 2021]. Specifically, aliphatic amines by gas-to-particle conversion are one candidate for WSON species observed in this study, as those amines of marine origin were observed in gas and aerosol phases in tropical and/or subtropical open oceans [e.g., Miyazaki et al., 2010; van Pinxteren et al., 2019]. Although the exact mechanism of the WSON formation is not apparent in this study, the current results of the shipboard measurements suggest that nitrogen fixation in SSW could partly explain one of the missing sources of atmospheric WSON and ammonia indicated by previous modeling studies.

To summarize, the current result suggests that  $\text{N}_2$ -fixing microorganisms in the SSW

likely contributed to the formation of aerosol WSON and possibly to other reactive nitrogen species, such as  $\text{NH}_3/\text{NH}_4^+$ , in the oceanic region of this study. Further field studies are required to elucidate the effect of nitrogen fixation in surface seawater on the emission of atmospheric reactive nitrogen in different oceanic regions. This includes, for example, simultaneous measurements of gas and particle phases of organic and inorganic nitrogen species together with measurements of biological and chemical parameters relevant to  $\text{N}_2$ -fixing microorganisms in surface seawater by shipboard observations. Additional laboratory studies are needed to evaluate the factors controlling the atmospheric emissions of reactive nitrogen associated with nitrogen fixation in surface seawater. Jiang et al. [2018] predicted that global ocean warming in the future would result in large increases in growth and nitrogen fixation by *Trichodesmium*. Consequently, the formation process and the amount of atmospheric WSON associated with nitrogen fixation in surface seawater are expected to change, which should be important from the viewpoints of the climate effect of marine atmospheric aerosols and of the air-sea exchange of nitrogen.

## **2.4 Conclusions**

This chapter investigated the origin and formation process of WSON aerosols in the oligotrophic subtropical North Pacific in terms of their linkage with  $\text{N}_2$ -fixing microorganisms in SSW based on the cruise measurements. The average concentration of

WSON in fine-mode aerosols along 23°N in the eastern North Pacific ( $7.5 \pm 6.6 \text{ ngN m}^{-3}$ ) was much higher than that in the western North Pacific ( $2.4 \pm 1.9 \text{ ngN m}^{-3}$ ) during the research cruise. The stable carbon isotope ratio of WSOC, together with backward trajectories, indicated that most of the observed WSON in the fine particles in the eastern North Pacific originated from the ocean surface. Relations of the concentrations of WSON with those of  $\text{Na}^+$  and MSA imply that secondary formation, which differed from the oxidation processes of DMS, was likely the dominant process underlying the formation of WSON observed in this study. Instead, significant positive correlations were found among nitrogen fixation rate, DON concentrations in SSW, and aerosol WSON concentrations. Meanwhile, the EC concentrations in all the samples were below the lower detection limit and did not show any statistically significant differences between WNP and ENP, suggesting that the effects of anthropogenic sources on the observed aerosols were likely small in this study. The overall results suggest that reactive nitrogen, such as dissolved organic nitrogen and ammonium, produced and exuded by nitrogen-fixing microorganisms in SSW, likely contributed to the formation of WSON aerosols over the oceanic region. This study provides new implications for the role of marine microbial activity in the formation of reactive nitrogen aerosols at the ocean surface.

## References

- Altieri, K. E., Fawcett, S. E., Peters, A. J., Sigman, D. M., and Hastings, M. G.: Marine biogenic source of atmospheric organic nitrogen in the subtropical North Atlantic, *Proc. Natl. Acad. Sci. U.S.A.*, 113, 925–930, <https://doi.org/10.1073/pnas.1516847113>, 2016.
- Altieri, K.E., Fawcett, S.E., and Hastings, M.G.: Reactive Nitrogen Cycling in the Atmosphere and Ocean, *Annu. Rev. Earth Planet. Sci.*, 49, 523–550, <https://doi.org/10.1146/annurev-earth-083120-052147>, 2021.
- Berthelot, H., Bonnet, S., Camps, M., Grosso, O., and Moutin, T.: Assessment of the dinitrogen released as ammonium and dissolved organic nitrogen by unicellular and filamentous marine diazotrophic cyanobacteria grown in culture, *Front Mar Sci*, 2, <https://doi.org/10.3389/fmars.2015.00080>, 2015.
- Bonnet, S., Biegala, I. C., Dutrieux, P., Slemmons, L. O., and Capone, D. G.: Nitrogen fixation in the western equatorial Pacific: rates, diazotrophic cyanobacterial size class distribution, and biogeochemical significance, *Glob. Biogeochem Cycles*, 23, GB3012, <https://doi.org/10.1029/2008GB003439>, 2009.
- Brüggemann, M., Hayeck, N. and George, C.: Interfacial photochemistry at the ocean surface is a global source of organic vapors and aerosols, *Nat. Commun.*, 9(1), 1–8, [doi:10.1038/s41467-018-04528-7](https://doi.org/10.1038/s41467-018-04528-7), 2018.
- Cachier, H., Buat-Ménard, M. P., Fontugne, M., and Chesselet, R.: Long-range transport of continentally derived particulate carbon in the marine atmosphere: evidence from stable isotope studies, *Tellus*, 38, 161–177, <https://doi.org/10.1111/j.1600-0889.1986.tb00184.x>, 1986.
- Capone, D. G., Ferrier, M. D., and Carpenter, E. J.: Cycling and release of glutamate and glutamine in colonies of the marine planktonic cyanobacterium, *Trichodesmium thiebautii*, *Appl. Environ. Microbiol.*, 60, 3989–3995, 1994.
- Carter, T. S., Joyce, E. E., Hastings, M. G.: Quantifying Nitrate Formation Pathways in the Equatorial Pacific Atmosphere from the GEOTRACES Peru-Tahiti Transect, *ACS Earth Space Chem.* 2021, 5, 10, 2638–2651, 2021.
- Cheung, S., Nitani, R., Tsurumoto, C., Endo, H., Nakaoka, S., Cheah, W., Lorda, J.F., Xia, X., Liu, H., and Suzuki, K.: Physical forcing controls the basin-scale occurrence

- of nitrogen-fixing organisms in the North Pacific Ocean, *Global Biogeochemical Cycles*, 34, e2019GB006452, <https://doi.org/10.1029/2019GB006452>, 2020.
- Dasari, S., Andersson, A., Bikkina, S., Holmstrand, H., Budhavant, K., Satheesh, S., Asmi, E., Kesti, J., Backman, J., Salam, A., Bisht, D. S., Tiwari, S., Hameed, Z., and Gustafsson, Ö.: Photochemical degradation affects the light absorption of water-soluble brown carbon in the South Asian outflow, *Sci. Adv.*, 5, eaau8066, <https://10.1126/sciadv.aau8066>, 2019.
- Duce, R.A., LaRoche, J., Altieri, K., Arrigo, K.R., Baker, A.R., Capone, D.G., Cornell, S., Dentener, F., Galloway, J., Ganeshram, R.S., Geider, R.J., Jickells, T., Kuypers, M.M., Langlois, R., Liss, P.S., Liu, S.M., Middelburg, J.J., Moore, C.M., Nickovic, S., Oschlies, A., Pedersen, T., Prospero, J., Schlitzer, R., Seitzinger, S., Sorensen, L.L., Uematsu, M., Ulloa, O., Voss, M., Ward, B., and Zamora, L.: Impacts of atmospheric anthropogenic nitrogen on the open ocean, *Science*, 320, 893–897, <https://doi.org/10.1126/science.1150369>, 2008.
- Dutheil, C., Aumont, O., Gorguès, T., Lorrain, A., Bonnet, S., Rodier, M., Dupouy, C., Shiozaki, T., and Menkes, C.: Modelling Nitrogen fixation related to *Trichodesmium* sp.: Driving processes and impacts on primary production in the tropical Pacific Ocean, *Biogeosciences*, 15(14), 4333–4352, <https://doi.org/10.5194/bg-15-4333-2018>, 2018.
- Facchini, M.C., Decesari, S., Rinaldi, M., Carbone, C., Finessi, E., Mircea, M., Fuzzi, S., Moretti, F., Tagliavini, E., Ceburnis, D., and O’Dowd, C.D.: Important Source of Marine Secondary Organic Aerosol from Biogenic Amines, *Environ. Sci. Technol.*, 42, 9116–9121, <https://doi.org/10.1021/es8018385>, 2008.
- Frischkorn, K. R., Haley, S. T., Dyhrman, S. T.: Coordinated gene expression between *Trichodesmium* and its microbiome over day–night cycles in the North Pacific Subtropical Gyre, *ISME Journal*, 12, 997–1007, <https://doi.org/10.1038/s41396-017-0041-5>, 2018.
- Hama, T., Miyazaki, T., Ogawa, Y., Iwakuma, T., Takahashi, M., Otsuki, A., and Ichimura, S.: Measurement of photosynthetic production of a marine phytoplankton population using a stable <sup>13</sup>C isotope, *Mar. Biol.*, 73, 31–36, <https://doi.org/10.1007/BF00396282>, 1983.
- Hashihama, F., Furuya, K., Kitajima, S., Takeda, S., Takemura, T., and Kanda, J.: Macro-

- scale exhaustion of surface phosphate by dinitrogen fixation in the western North Pacific, *Geophys. Res. Lett.*, 36, L03610, doi:10.1029/2008GL036866, 2009.
- Hashihama, F., Kanda, J., Tauchi, A., Kodama, T., Saito, H., and Furuya, K.: Liquid waveguide spectrophotometric measurement of nanomolar ammonium in seawater based on the indophenol reaction with o-phenylphenol (OPP), *Talanta*, 143, 374–380, 2015.
- Hashihama, F., Saito, H., Shiozaki, T., Ehama, M., Suwa, S., Sugiyama, T., Kato, H., Kanda, J., Sato, M., Kodama, T., Yamaguchi, T., Horii, S., Tanita, I., Takino, S., Takahashi, K., and Ogawa, H.: Biogeochemical controls of particulate phosphorus distribution across the oligotrophic subtropical Pacific Ocean, *Glob. Biogeochem. Cycles*, 34, e2020GB006669, <https://doi.org/10.1029/2020GB006669>, 2020.
- Horii, S., Takahashi, K., Shiozaki, T., Hashihama, F., and Furuya, K.: Stable isotopic evidence for differential contribution of diazotrophs to the epipelagic grazing food chain in the mid-Pacific Ocean, *Global Ecol. Biogeogr.*, 27, 1467–1480, <https://doi.org/10.1111/geb.12823>, 2018.
- Jiang, H. B., Fu, F. X., Rivero-Calle, S., Levine, N. M., Sañudo-Wilhelmy, S. A., Qu, P. P., Wang, X. W., Pinedo-Gonzalez, P., Zhu, Z., and Hutchins, D. A.: Ocean warming alleviates iron limitation of marine nitrogen fixation, *Nature Climate Change*, 8, 709–712, <https://doi.org/10.1038/s41558-018-0216-8>, 2018.
- Jickells, T. D., Kelly, S. D., Baker, A. R., Biswas, K., Dennis, P. F., Spokes, L. J., Witt, M., and Yeatman, S. G.: Isotopic evidence for a marine ammonia source, *Geophys. Res. Lett.*, 30, 1374, <https://doi.org/10.1029/2002GL016728>, 2003.
- Johnson, M. T., Liss, P. S., Bell, T. G., Lesworth, T. J., Baker, A. R., Hind, A. J., Jickells, T. D., Biswas, K. F., Woodward, E. M. S., and Gibb, S. W.: Field observations of the ocean-atmosphere exchange of ammonia: Fundamental importance of temperature as revealed by a comparison of high and low latitudes, *Global Biogeochemical Cycles*, 22, GB1019, <https://doi.org/10.1029/2007GB003039>, 2008.
- Kamezaki, K., Hattori, S., Iwamoto, Y., Ishino, S., Furutani, H., Miki, Y., Uematsu, M., Miura, K., and Yoshida, N.: Tracing the sources and formation pathways of atmospheric particulate nitrate over the Pacific Ocean using stable isotopes, *Atmos. Environ.*, 209, 152–166, <https://doi.org/10.1016/J.ATMOSENV.2019.04.026>, 2019.

- Kanakidou, M., Duce, R. A., Prospero, J. M., Baker, A. R., Benitez-Nelson, C., Dentener, F. J., Hunter, K. A., Liss, P. S., Mahowald, N., Okin, G. S., Sarin, M., Tsigaridis, K., Uematsu, M., Zamora, L. M., Zhu, T.: Atmospheric fluxes of organic N and P to the global ocean, *Global Biogeochem Cycles*, 26, GB3026, <https://doi.org/10.1029/2011GB004277>, 2012.
- Karl, D. M., Letelier, R., Hebel, D. V., Bird, D. F., and Winn, C. D.: *Trichodesmium* blooms and new nitrogen in the north Pacific gyre, p. 219-237, *Marine pelagic cyanobacteria: Trichodesmium and other diazotrophs*. Kluwer Academic Publishers, Dordrecht, The Netherlands, 1992.
- Konno, U., Tsunogai, U., Komatsu, D. D., Daita, S., Nakagawa, F., Tsuda, A., Matsui, T., Eum, Y.-J., and Suzuki, K.: Determination of total N<sub>2</sub> fixation rates in the ocean taking into account both the particulate and filtrate fractions. *Biogeosciences*, 7, 2369–2377. doi: 10.5194/bg-7-2369-2010, 2010.
- Letelier, R. M. and Karl, D. M.: The role of *Trichodesmium* spp. In the productivity of the subtropical North Pacific Ocean, *Mar. Ecol. Prog. Ser.*, 133, 263-273, 1994.
- Luo, Y. W., Lima, I. D., Karl, D. M., Deutsch, C. A. and Doney, S. C.: Data-based assessment of environmental controls on global marine nitrogen fixation, *Biogeosciences*, 11, 691–708, <https://doi.org/10.5194/bg-11-691-2014>, 2014.
- Miyazaki, Y., Kawamura, K., Jung, J., Furutani, H., and Uematsu, M.: Latitudinal distributions of organic nitrogen and organic carbon in marine aerosols over the western North Pacific, *Atmos. Chem. Phys.*, 11, 3037–3049, <https://doi.org/10.5194/acp-11-3037-2011>, 2011.
- Miyazaki, Y., P.Q. Fu, Kawamura, K., Mizoguchi, Y., and Yamanoi, K.: Seasonal variations of stable carbon isotopic composition and biogenic tracer compounds of water-soluble organic aerosols in a deciduous forest, *Atmos. Chem. Phys.*, 12, 1367–1376, <https://doi.org/10.5194/acp-12-1367-2012>, 2012.
- Miyazaki, Y., Coburn, S., Ono, K., Ho, D. T., Pierce, R. B., Kawamura, K., and Volkamer, R.: Contribution of dissolved organic matter to submicron water-soluble organic aerosols in the marine boundary layer over the eastern equatorial Pacific, *Atmos. Chem. Phys.*, 16, 7695–7707, <https://doi.org/10.5194/acp-16-7695-2016>, 2016.
- Miyazaki, Y., Yamashita, Y., Kawana, K., Tachibana, E., Kagami, S., Mochida, M., Suzuki,

- K. and Nishioka, J.: Chemical transfer of dissolved organic matter from surface seawater to sea spray water-soluble organic aerosol in the marine atmosphere, *Sci. Rep.*, 8, 14861, <https://doi.org/10.1038/s41598-018-32864-7>, 2018.
- Mohr, W., Großkopf, T., Wallace, D. W. R., and Laroche, J.: Methodological underestimation of oceanic nitrogen fixation rates, *PLoS ONE*, 5, <https://doi.org/10.1371/journal.pone.0012583>, 2010.
- Mohr, C., Lopez-Hilfiker, F. D., Zotter, P., Prévôt, A. S. H., Xu, L., Ng, N. L., Herndon, S. C., Williams, L. R., Franklin J. P., Zahniser, M. S., Worsnop, D. R., Knighton, W. B., Aiken, A. C., Gorkowski, K. J., Dubey M. K., Allan J. D., and Thornton, J. A.: Contribution of nitrated phenols to wood burning brown carbon light absorption in Detling, United Kingdom during wintertime, *Environ. Sci. Technol.*, 47, 6316–6324, <https://doi.org/10.1021/es400683v>, 2013.
- Montoya, J. P., Voss, M., Kaehler, P., and Capone, D. G.: A simple, high precision, high sensitivity tracer assay for dinitrogen fixation, *Appl. Environ. Microbiol.*, 62, 986–993, <https://doi.org/10.1128/AEM.62.3.986-993.1996>, 1996.
- Montoya, J. P., Holl, C. M., Zehr, J. P., Hansen, A., Villareal, T. A. and Capone, D. G.: High rates of Nitrogen fixation by unicellular diazotrophs in the oligotrophic Pacific Ocean, *Nature*, 430, 1027–1032, <https://doi.org/10.1038/nature02824>, 2004.
- Mungall, E. L., Wong, J. P. S., Abbatt, P. D.: Heterogeneous oxidation of particulate methanesulfonic acid by the hydroxyl radical: kinetics and atmospheric implications, *ACS Earth Space Chem.* 2018, 2, 48–55, 2018.
- Nehir, M. and Koçak, M.: Atmospheric water-soluble organic nitrogen (WSON) in the eastern Mediterranean: origin and ramifications regarding marine productivity, *Atmos. Chem. Phys.*, 18, 3603–3618, <https://doi.org/10.5194/acp-18-3603-2018>, 2018.
- Oreopoulos, L., and Platnick, S.: Radiative susceptibility of cloudy atmospheres to droplet number perturbations. II. Global analysis from MODIS, *J. Geophys. Res.*, 113, D14S21, <https://doi.org/10.1029/2007JD009655>, 2008.
- Ottesen, E. A., Young, C. R., Gifford, S. M., Eppley, J. M., Marin, R. 3rd, Schuster, S. C., Scholin, C. A. and DeLong, E. F.: Ocean microbes. Multispecies diel transcriptional oscillations in open ocean heterotrophic bacterial assemblages, *Science*, 345, 207–212, <https://doi.org/10.1126/science.1252476>, 2014.



- Paulot, F., Jacob, D. J., Johnson, M. T., Bell, T. G., Baker, A. R., Keene, W. C., Lima, I. D., Doney, S. C., and Stock, C. A.: Global oceanic emission of ammonia: Constraints from seawater and atmospheric observations, *Global Biogeochem. Cycles*, 29, 1165–1178, <https://doi.org/10.1002/2015GB005106>, 2015.
- Rosenfeld, D., Zhu, Y. N., Wang, M. H., Zheng, Y. T., Goren, T., and Yu, S. C.: Aerosol-driven droplet concentrations dominate coverage and water of oceanic low level clouds, *Science*, 363, eaav0566, <https://doi.org/10.1126/science.aav0566>, 2019.
- Rousseaux, C. S., and Gregg, W. W.: Climate variability and phytoplankton composition in the Pacific Ocean, *J. Geophys. Res.*, 117, C10006, <https://doi.org/10.1029/2012JC008083>, 2012.
- Salter, S., Sortino, G., and Latham, J.: Sea-going hardware for the cloud albedo method of reversing global warming, *Philos. T. Roy. Soc. A*, 366, 3989–4006, <https://doi.org/10.1098/rsta.2008.0136>, 2008.
- Shiozaki, T., Bombar, D., Riemann, L., Hashihama, F., Takeda, S., Yamaguchi, T., Ehoma, M., Hamasaki, K., Furuya, K.: Basin scale variability of active diazotrophs and nitrogen fixation in the North Pacific, from the tropics to the subarctic Bering Sea, *Global Biogeochemical Cycles*, 31, 996–1009, <https://doi.org/10.1002/2017GB005681>, 2017.
- Shiozaki, T., Bombar, D., Riemann, L., Sato, M., Hashihama, F., Kodama, T., Tanita, I., Takeda, S., Saito, H., Hamasaki, K., Furuya, K.: Linkage between dinitrogen fixation and primary production in the oligotrophic South Pacific Ocean, *Global Biogeochemical Cycles*, 32, 1028–1044, <https://doi.org/10.1029/2017GB005869>, 2018.
- Suzuki, R. and Ishimaru, T.: An improved method for the determination of phytoplankton chlorophyll using N, N-dimethylformamide, *J. Oceanog.*, 46(4):190–194, <https://doi.org/10.007/BF02125580>, 1990.
- van Pinxteren, M., Barthel, S., Fomba, K. W., Müller, K., von Tümpling, W., and Herrmann, H.: The influence of environmental drivers on the enrichment of organic carbon in the sea surface microlayer and in submicron aerosol particles-Measurements from the Atlantic Ocean, *Elementa Science of the Anthropocene*, 5, 35, <https://doi.org/10.1525/elementa.225>, 2017.

- Wang, W. L., Moore, J. K., Martiny, A. C., and Primeau, F. W.: Convergent estimates of marine nitrogen fixation, *Nature*, 566, 205–211, <https://doi.org/10.1038/s41586-019-0911-2>, 2019.
- Wannicke, N., Koch, B. P., and Voss, M.: Release of fixed N<sub>2</sub> and C as dissolved compounds by *Trichodesmium erythreum* and *Nodularia spumigena* under the influence of high light and high nutrient (P), *Aquat Microb Ecol*, 57, 175–189, <https://doi.org/10.3354/ame01343>, 2009.
- Yamaguchi, T., Sato, M., Hashihama, F., Ehama, M., Shiozaki, T., Takahashi, K., and Furuya, K.: Basin-scale variations in labile dissolved phosphoric monoesters and diesters in the central North Pacific Ocean, *J. Geophys. Res.: Oceans*, 124, 3058–3072, <https://doi.org/10.1029/2018jc014763>, 2019.
- Yamaguchi, T., Sato, M., Hashihama, F., Kato, H., Sugiyama, T., Ogawa, H., Takahashi, K., and Furuya, K.: Longitudinal and vertical variations of dissolved labile phosphoric monoesters and diesters in the subtropical North Pacific, *Front. Microbiol.*, 11, 570081, <https://doi.org/10.3389/fmicb.2020.570081>, 2021.
- Yasui-Tamura, S., Hashihama, F., Ogawa, H., Nishimura, T., and Kanda, J.: Automated simultaneous determination of total dissolved nitrogen and phosphorus in seawater by persulfate oxidation method, *Talanta Open*, 2, 100016, <https://doi.org/10.1016/j.talo.2020.100016>, 2020.
- Yvon-Durocher, G., Dossena, M., Trimmer, M., Woodward, G., and Allen, A. P.: Temperature and the biogeography of algal stoichiometry, *Global Ecology and Biogeography*, 24, 562–570, <https://doi.org/10.1111/geb.12280>, 2015.
- Zehr, J. P. and Capone, D. G.: Changing perspectives on nitrogen fixation, *Science*, 368, eaay9514, <https://doi.org/10.1126/science.aay9514>, 2020.
- Zhu, L., Nenes, A., Wine, P. H., and Nicovich, J. M.: Effects of aqueous organosulfur chemistry on particulate methanesulfonate to nonsea salt sulfate ratios in the marine atmosphere, *J. Geophys. Res.* 111, D05316, <https://doi.org/10.1029/2005JD006326>, 2006.

**Table 2.1** Average concentrations of nitrogen species and stable carbon isotope ratios in the fine ( $D_p < 0.95 \mu\text{m}$ ) and coarse ( $D_p > 0.95 \mu\text{m}$ ) aerosol particles collected along  $23^\circ\text{N}$  in each oceanic region.

	The western North Pacific (WNP, $135\text{--}200^\circ\text{E}$ )		The eastern North Pacific (ENP, $200\text{--}240^\circ\text{E}$ )		All ( $135\text{--}240^\circ\text{E}$ )	
	Fine	Coarse	Fine	Coarse	Fine	Coarse
WSON ( $\text{ngN m}^{-3}$ )	$2.4\pm 1.9$	$7.9\pm 6.0$	$7.5\pm 6.6$	$49.0\pm 12.6$	$6.1\pm 6.2$	$21.6\pm 21.3$
$\text{NH}_4^+$ ( $\text{ngN m}^{-3}$ )	$42.6\pm 15.8$	$3.6\pm 3.2$	$35.5\pm 22.2$	$17.5\pm 8.3$	$37.4\pm 20.9$	$8.3\pm 8.5$
$\text{NO}_3^-$ ( $\text{ngN m}^{-3}$ )	$0.5\pm 0.4$	$154.6\pm 65.8$	$1.8\pm 1.8$	$373.2\pm 91.1$	$1.5\pm 1.7$	$227.5\pm 127.6$
$\text{NO}_2^-$ ( $\text{ngN m}^{-3}$ )	$0.4\pm 0.2$	$32.9\pm 54.0$	$1.4\pm 1.4$	$9.4\pm 9.4$	$1.1\pm 1.3$	$25.0\pm 45.8$
nss- $\text{Ca}^{2+}$ ( $\text{ng m}^{-3}$ )	$1.6\pm 1.5$	$166.4\pm 81.5$	$0.4\pm 1.1$	$211.8\pm 4.3$	$0.7\pm 1.3$	$181.5\pm 69.9$
nss- $\text{K}^+$ ( $\text{ng m}^{-3}$ )	$5.2\pm 4.8$	$120.5\pm 60.7$	$3.9\pm 3.0$	$141.8\pm 9.9$	$4.2\pm 3.6$	$127.6\pm 50.9$
nss- $\text{SO}_4^{2-}$ /MSA	$5.5\pm 3.6$	$11.4\pm 3.5$	$4.7\pm 7.2$	$19.5\pm 10.6$	$4.9\pm 6.4$	$14.1\pm 7.8$
$\delta^{13}\text{C}_{\text{wsoc}}$ (‰)	$-23.9\pm 1.4$	NA	$-22.1\pm 1.6$	NA	$-22.8\pm 1.7$	NA

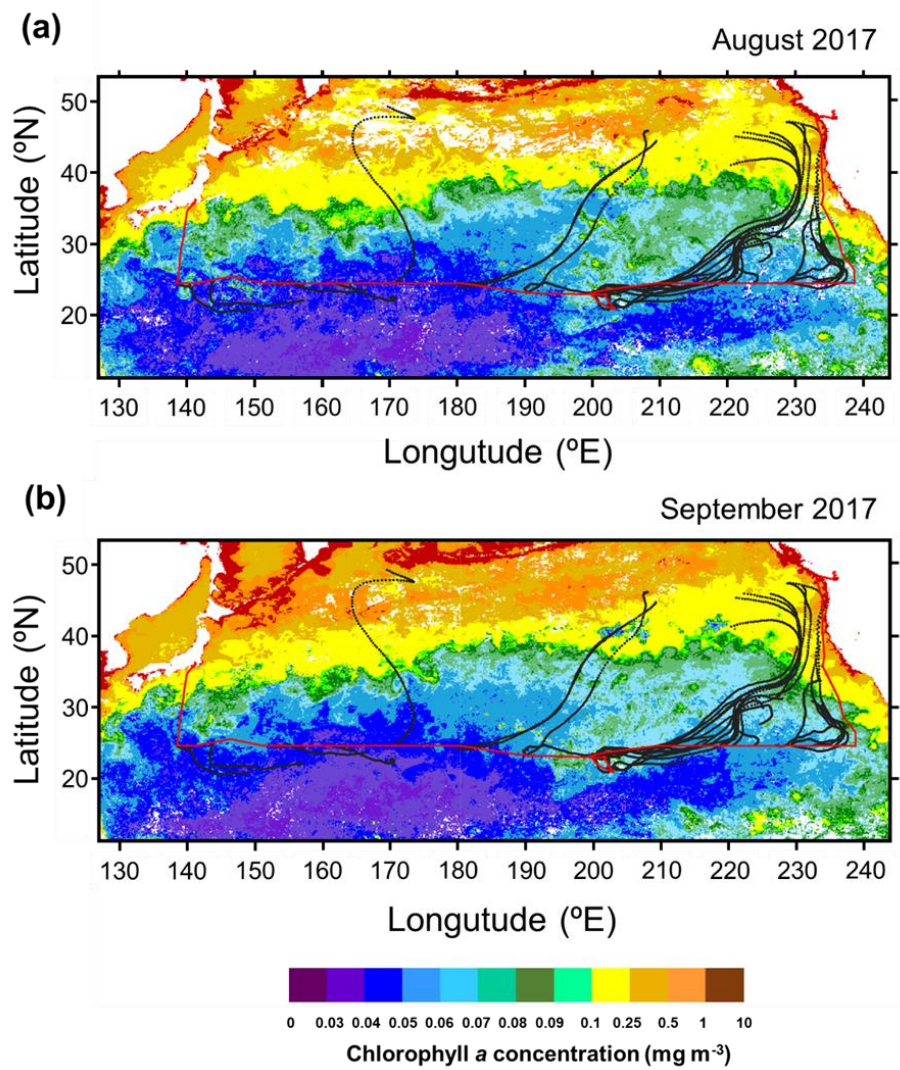


**Figure 2.1** *R/V Hakuho Maru* cruise track in the subtropical North Pacific between 12 August and 5 October 2017 (red), together with typical 5-day back trajectories (black). Also shown are monthly averaged concentrations of Chl-*a* for (a)

August and (b) September 2017 derived from the MODIS-Aqua ([https://neo.sci.gsfc.nasa.gov/view.php?datasetId=MY1DMM\\_CHLORA&year=2017](https://neo.sci.gsfc.nasa.gov/view.php?datasetId=MY1DMM_CHLORA&year=2017)). The area in which data are missing is shown in white.

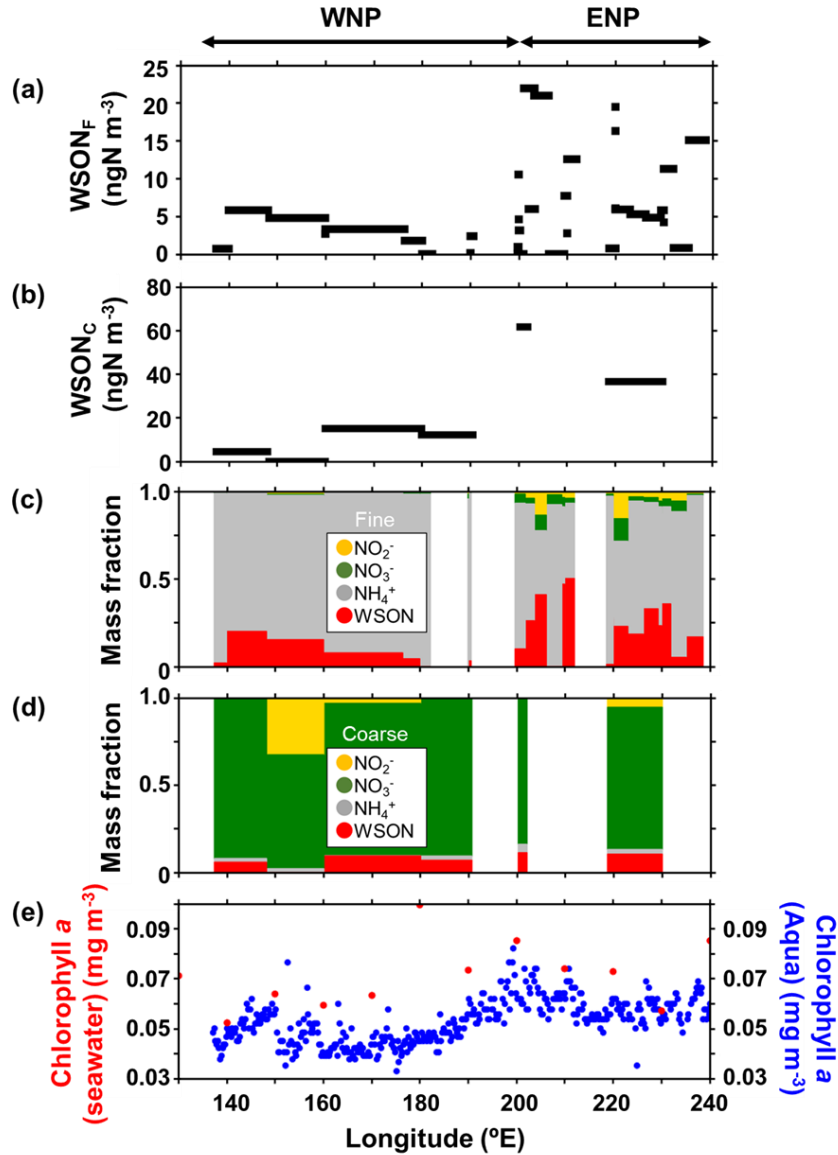


**Figure 2.2** Longitudinal distributions of each parameter of the atmospheric aerosols and surface seawater along 23°N; the mass concentrations of WSON in (a) fine particles (WSON<sub>F</sub>) and (b) coarse particles (WSON<sub>C</sub>); the chemical mass fractions of nitrogen species in (c) WSON<sub>F</sub> and (d) WSON<sub>C</sub>; (e) Chl-*a* concentrations in the surface seawater samples during the cruise (red) and the average Chl-*a* concentrations from August–September 2017, as measured by

MODIS-Aqua (blue). WNP and ENP denote the oceanic regions of the western North Pacific and eastern North Pacific, respectively, defined in this study.

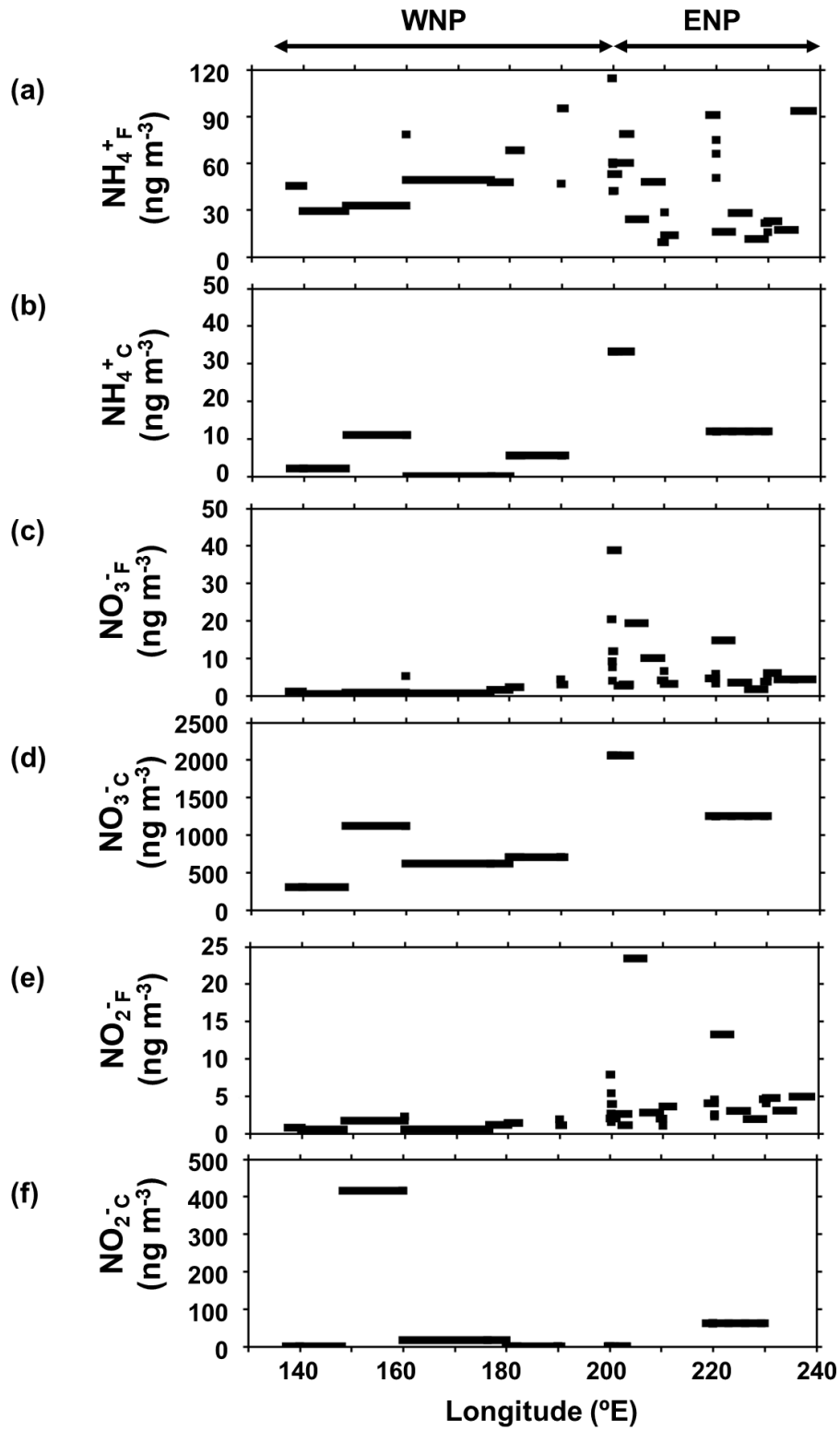


**Figure 2.3** Longitudinal distributions of mass concentrations of (a)  $\text{NH}_4^+_{\text{F}}$ , (b)  $\text{NH}_4^+_{\text{C}}$ , (c)  $\text{NO}_3^-_{\text{F}}$ , (d)  $\text{NO}_3^-_{\text{C}}$ , (e)  $\text{NO}_2^-_{\text{F}}$ , and (f)  $\text{NO}_2^-_{\text{C}}$  along  $23^\circ\text{N}$ .

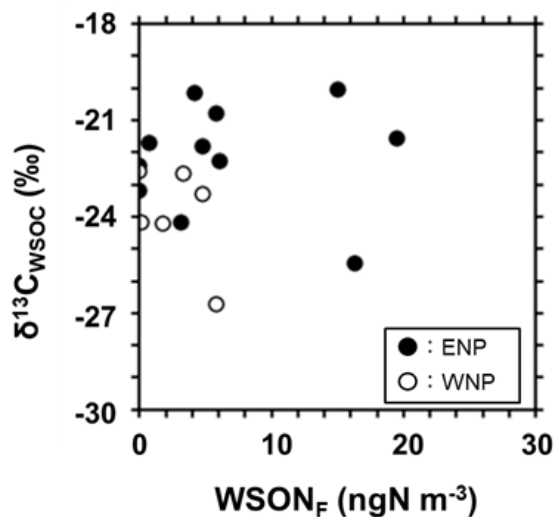


**Figure 2.4**  $\delta^{13}\text{C}$  of WSOC ( $\delta^{13}\text{C}_{\text{WSOC}}$ ) as a function of the concentrations of  $\text{WSON}_{\text{F}}$ . Solid and open circles indicate the data of the eastern North Pacific (ENP;  $200\text{--}240^\circ\text{E}$ ) and the western North Pacific (WNP;  $135\text{--}200^\circ\text{E}$ ), respectively.

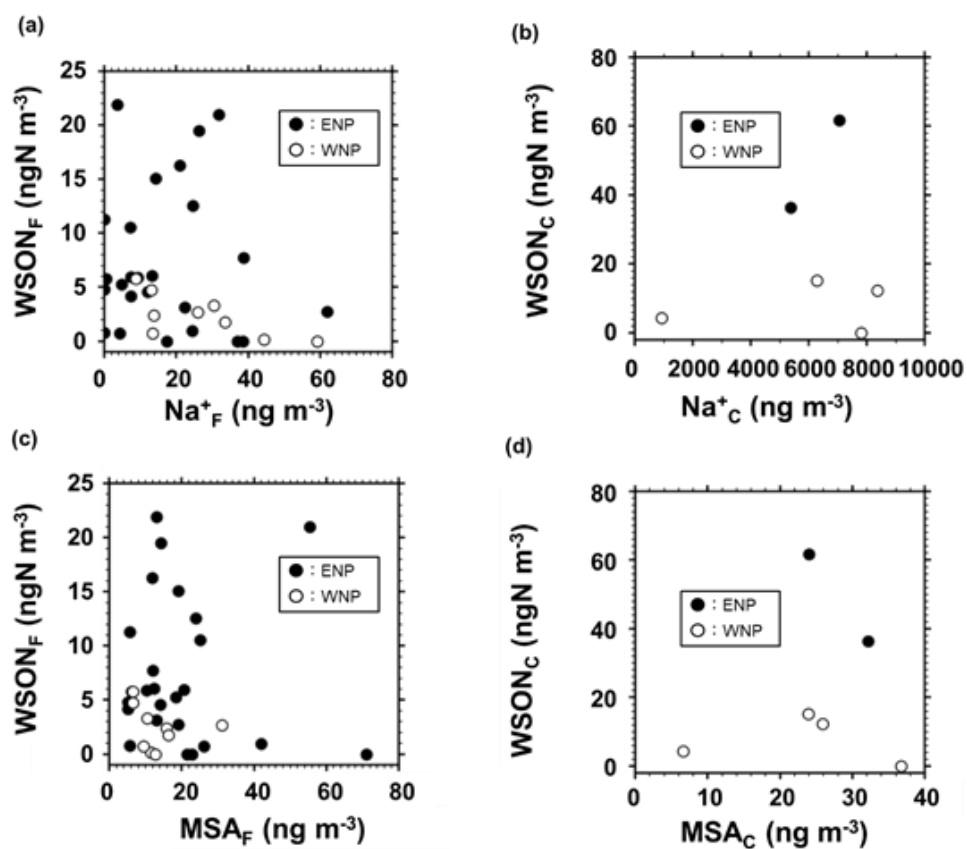


**Figure 2.5** Concentrations of WSON as functions of those of sodium (a, b) and MSA (c, d), where (a) and (c) are for the fine particles and (b) and (d) are for the coarse particles. Solid and open circles represent the data of the eastern North Pacific (ENP) and western North Pacific (WNP), respectively.



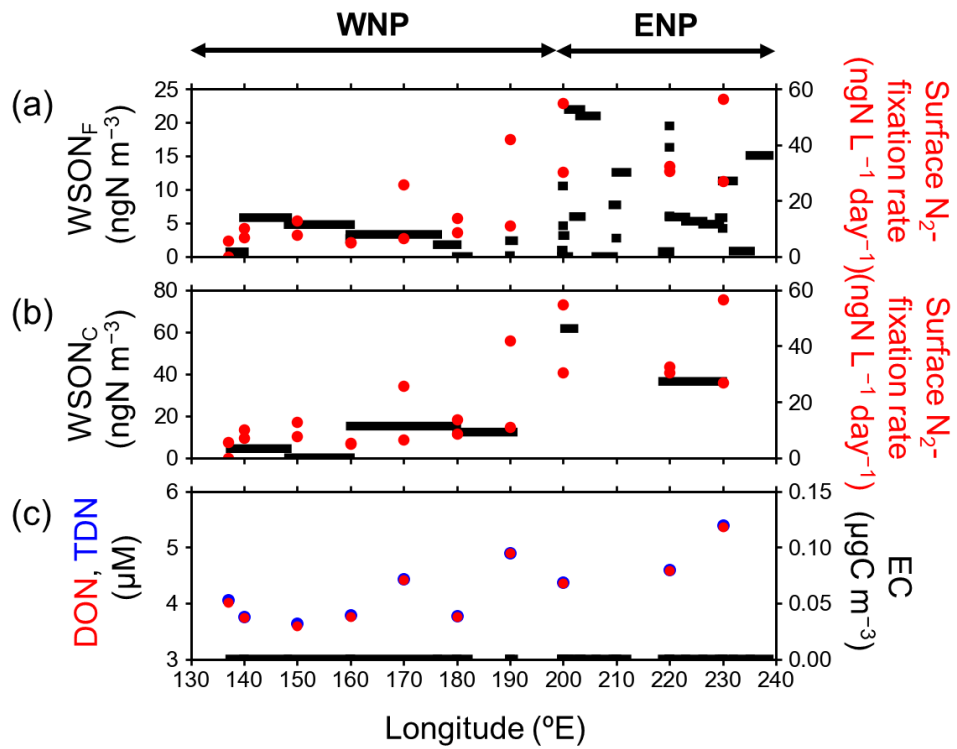


**Figure 2.6** Longitudinal distributions of mass concentrations of (a)  $WSON_F$  (black) and (b)  $WSON_C$  (black), together with nitrogen fixation rate in the SSW samples (solid red circle), and (c) DON (solid red circle) and TDN (solid blue circle) concentrations in surface seawater and aerosol EC concentrations (black) during the entire cruise.

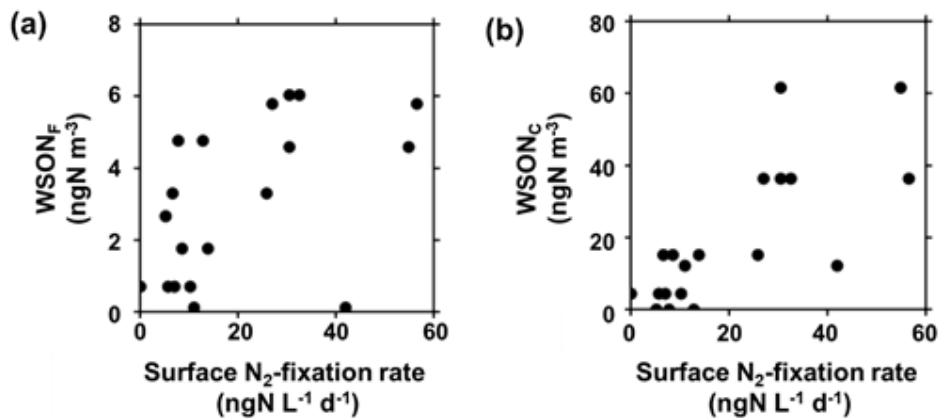


**Figure 2.7** Mass concentrations of (a) WSON<sub>F</sub> and (b) WSON<sub>C</sub> as a function of nitrogen fixation rate in SSW. The data of nitrogen fixation rate in SSW were merged into the duration of each corresponding aerosol sampling. For each one aerosol sample, one or more corresponding measurement data of nitrogen fixation rate in SSW were obtained, so that the number of the data points in the panels is more than that of the aerosol samples.

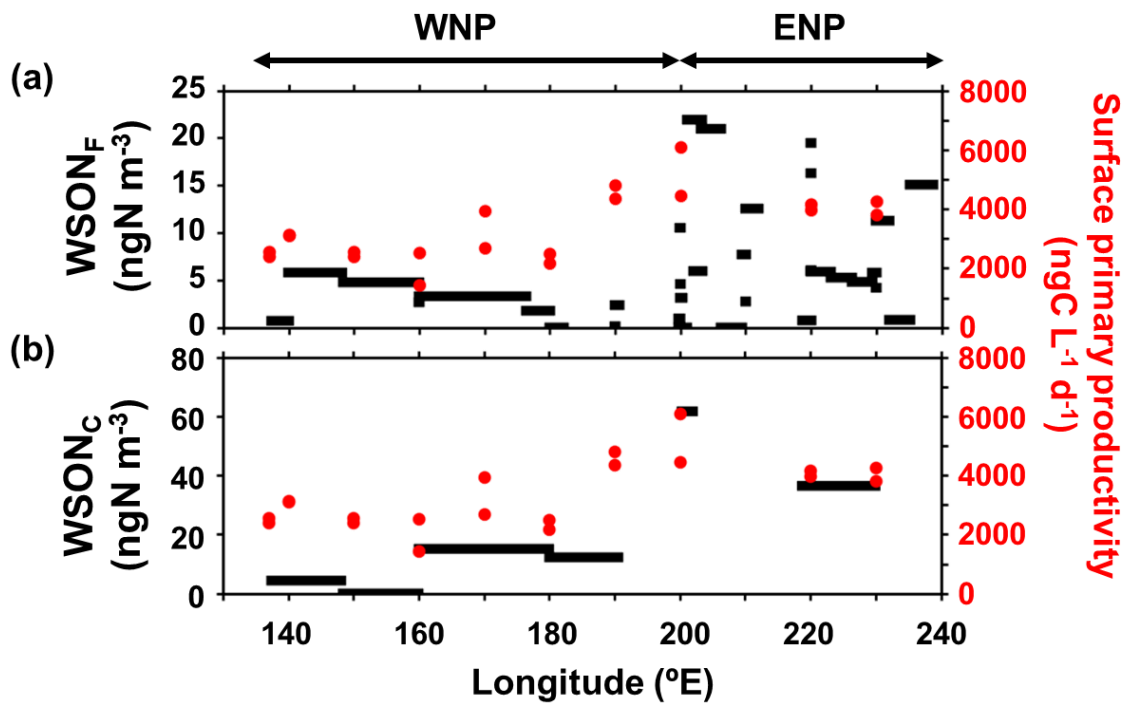


**Figure 2.8** Longitudinal distributions of mass concentrations of (a)  $WSON_F$  and (b)  $WSON_C$ , together with primary productivity in the SSW samples during the entire cruise.

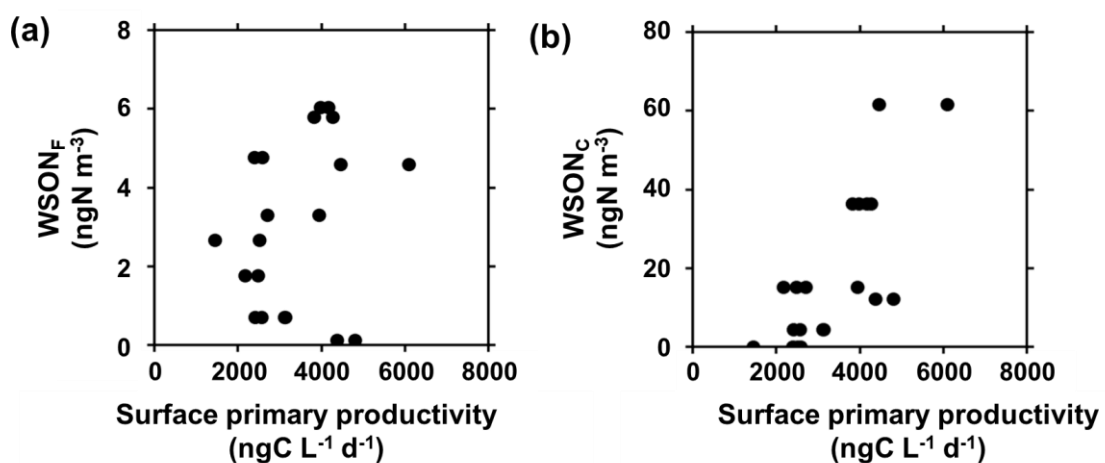


**Figure 2.9** The mass concentrations of (a)  $WSON_F$  and (b)  $WSON_C$  as a function of primary productivity in SSW.

# **Chapter 3. Effects of Marine Nitrogen Fixation on Atmospheric Emissions of Reactive Nitrogen Revealed by a Laboratory Incubation Experiment**

## **3.1 Introduction**

This chapter shows the results of an incubation experiment in a laboratory to prove that atmospheric reactive nitrogen, including WSON, is indeed emitted from seawater associated with marine nitrogen fixation, as suggested in Chapter 2. Previous laboratory studies on sea-to-air emissions of biochemical and microbiological components have mainly focused on organic matter in sea spray aerosols and the gas phase associated with microbes. For example, Rastelli et al. [2017] simulated the emission of airborne sea sprays through bubble-bursting experiments using the seawater of the North-Eastern Atlantic Ocean offshore Ireland. They showed that the submicrometer aerosol of primary emissions was highly enriched in organic matter such as lipids, proteins, and carbohydrates compared with seawater. Their results suggested that enhanced biological activity and the release of lipid compounds at the sea surface can significantly increase the carbon content of the emitted marine aerosols. Bernard et al. [2016] focused on abiotic processes emitted as gases from the sea-surface microlayer (SML) through photochemical reactions, followed by particle formations in the atmosphere. They used a multiphase

atmospheric simulation chamber to show that not only marine secondary organic aerosols (SOA) derived from gases released by microorganisms but also the process of becoming SOA by photochemical reactions in the SML is important.

To the author's knowledge, no experiments have been conducted so far to incubate nitrogen-fixing microorganisms with a simultaneous atmospheric observation of gases and particles emitted from seawater. Based on the results shown in Chapter 2, this chapter aims to elucidate the contribution of nitrogen-fixing microorganisms to the formation of atmospheric reactive nitrogen, including WSON, by a laboratory incubation experiment. In this study, *Trichodesmium* was chosen as a representative of nitrogen-fixing microorganisms for the experiment. *Trichodesmium* is widely distributed in the tropical and subtropical oceans [Zehr and Capone., 2020]. *Trichodesmium* contributes to ~50% (or more) of the total amount of nitrogen fixed by nitrogen fixation in the global ocean [Mahaffey et al., 2005; Westberry et al., 2006]. *Trichodesmium* was incubated in artificial seawater with continuous atmospheric samplings of particulate and gas-phase reactive nitrogen together with seawater sampling once a day.

## **3.2 Experimental method**

### **3.2.1 Incubation of *Trichodesmium* with artificial seawater and atmospheric sampling system**

**Figure 3.1** shows an experimental system set up for incubating nitrogen-fixing

cyanobacterium *Trichodesmium* followed by collecting atmospheric and seawater samples. In this experiment, *Trichodesmium erythraeum* IMS101 (hereafter described as *Trichodesmium*) was incubated in an acrylic tank containing approximately 20 L of artificial seawater under conditions of controlled temperature and light intensity by using an incubator and fluorescent lamps (FL40S.BRN plantlaks, TOSHIBA Corp.) with the visible wavelength range. The light condition also enables photochemical reaction in the atmosphere and seawater. Atmospheric samples were collected continuously for 24 hours, while seawater samples were collected once per ~24 hours. Details of each sampling are given in the following sections. The incoming air from outside the tank was filtered with an air filter (Disposable Adsorption Units, Balston) that can absorb gases (e.g., ethylene, propylene, and ammonia) to reduce any contamination that entered the tank.

### **3.2.2 Incubation condition**

In this experiment, artificial-seawater-based YBC-II [Chen et al. 1996], free of reactive nitrogen, was used as a culture medium for the incubation of *Trichodesmium*. Incubation was conducted in this medium at 25°C with a daily cycle of light intensity: 195  $\mu\text{mol photon m}^{-2} \text{ s}^{-1}$  for 12 hours and another 12 hours in the dark. Temperature and light intensity were set to make optimal conditions for the growth of *Trichodesmium* based on the previous incubation experiment [Boatman et al., 2017].

### 3.2.3 Atmospheric sampling

Atmospheric samples were collected at a flow rate of  $20 \text{ L min}^{-1}$  with a NILU impactor (Tokyo Dylec. Corp.). The flow rate was controlled by a volumetric flow meter with the integrated sampling volume monitored. The NILU impactor consists of four impaction stages. The first top stage collected particles with particle diameter ( $D_p$ ) larger than  $2.5 \mu\text{m}$ , the sample of which was not used in this study, because the larger particles could not be collected by the impactor in the experimental setup. For the second stage, particles with  $D_p < 2.5 \mu\text{m}$  was collected on quartz fiber filters with an effective diameter of  $47 \text{ mm}$ ). The third and fourth stages collected acidic and basic gases onto a cellulose filter impregnated with 2% sodium carbonate ( $\text{NaCO}_3$ ) and 2% phosphoric acid, respectively. Before the sampling, the cellulose filter was stored at  $-20 \text{ }^\circ\text{C}$  in a freezer to prevent drying of the impregnation.

Prior to the incubation of *Trichodesmium*, atmospheric samples were collected under conditions with no *Trichodesmium* in seawater. These filter samples were used as blank field filters to determine the concentrations of each chemical parameter. That is, the concentration of the field blank was subtracted from that of the samples collected during the incubation of *Trichodesmium*.

### 3.2.4 Artificial seawater sampling

Artificial seawater was collected once per 24 hours. For *in vivo* fluorescence intensity

measurements, 1 ml of seawater was collected every day during the incubation. For the measurement of chlorophyll *a* (Chl-*a*) concentration, 50 ml × 2 seawater samples were collected eight times throughout the experiment. In addition, eighteen samples of 1 ml seawater were collected to measure bacteria concentration during the period. All of these seawater samples were collected using a peristaltic pump.

### **3.2.5 Chemical analysis of atmospheric samples**

To measure the mass concentrations of water-soluble organic carbon (WSOC) and water-soluble total nitrogen (WSTN) in the filter samples, a filter cut of 6.28 cm<sup>2</sup> was extracted with 15 mL of ultrapure water under ultrasonication and filtered using a disc filter (Millex-GV, 0.22 μm, Millipore, Billerica, MA, USA). The concentrations of WSOC and WSTN were determined using a total organic carbon (TOC) analyzer with a TN unit (Model TOC-L<sub>CHP</sub>+TNM-L, SHIMADZU).

Another cut of the filter (6.28 cm<sup>2</sup>) was extracted with 7 or 50 mL of ultrapure water to measure the concentrations of NH<sub>4</sub><sup>+</sup>, NO<sub>3</sub><sup>-</sup>, and NO<sub>2</sub><sup>-</sup>. The same syringe filter type as described above was used, before the extract was injected into an ion chromatograph (Model 761 compact IC; Metrohm). The WSON concentration was defined as the difference between the WSTN and inorganic nitrogen (NH<sub>4</sub><sup>+</sup>, NO<sub>3</sub><sup>-</sup>, and NO<sub>2</sub><sup>-</sup>) concentrations.



### **3.2.6 Measurements of chemical and biological parameters of artificial seawater**

To measure the concentrations of dissolved organic carbon (DOC) and dissolved nitrogen (DN) in the seawater samples, 7.5 ml of the sample was filtered using a disc filter (Millex-GV, 0.22  $\mu\text{m}$ , Millipore, Billerica, MA, USA). The filtered seawater sample was diluted with 7.5 ml of ultrapure water. A total of 15 ml sample was used for the determination of the DOC and DN concentrations by using a total organic carbon (TOC) analyzer with a TN unit (Model TOC-L<sub>CHP</sub>+TNM-L, SHIMADZU).

*In vivo* fluorescence intensity in 1-ml seawater samples was measured by Qubit® 2.0 Fluorometer (Thermo Fisher SCIENTIFIC) every day of the experiment. Phytoplankton pigment (Chl-*a* concentration) was measured using ultra-high performance liquid chromatography (Shimazu UHPLC Nexera X2) [Suzuki et al., 2015]. The measurement data showed a linear relationship between the *in vivo* fluorescence intensity and Chl-*a* concentration. Chl-*a* concentration for all the samples was then calculated with a linear regression line from the *in vivo* fluorescence intensity. To measure bacteria concentration, another 1-ml seawater sample was put into a cryovial containing 20  $\mu\text{L}$  of 10% PFA (paraformaldehyde), which was stored at  $-80\text{ }^{\circ}\text{C}$  until the analysis. Bacteria concentration was then measured using a flow cytometer (BD FACSCantoTMII).

## **3.3 Results and discussion**

### 3.3.1 Definition of growth phases of *Trichodesmium*

**Figure 3.3** shows the observed temporal variations in the concentrations of Chl-*a* and bacteria in seawater during an incubation period of about 2 months. Here, Day 0 is defined as the date when *Trichodesmiumn* was put into the culture medium to start the monitoring. Chl-*a* concentration started to increase after Day 20, reaching the maximum concentration of 106.4 mg m<sup>-3</sup> on Day 30. Then the concentration showed a decrease until Day 48.

To define each period of the growth and decline stages in *Trichodesmiumn*, a growth rate (GR) of *Trichodesmiumn* was calculated using the following equation:

$$\text{GR} = \frac{\log (C_{(t)}) - \log (C_{(t_0)})}{t - t_0} \times 1000$$

where  $C_{(t)}$  and  $C_{(t_0)}$  denote concentrations of Chl-*a* at a start time ( $t_0$ ) and end time ( $t$ ) of each seawater sampling, respectively. **Figure 3.4** presents the temporal changes in the growth rate with the 5-day running-mean values (**Table 3.1**). First, a period when the Chl-*a* concentrations was below 2.0 mg m<sup>-3</sup> (Days 0–21) was defined as the lag phase. The exponential phase was set when GR was greater than 1.5 (Days 21–29). The stationary phase was defined as a period when GR was between –6 and 1.5 (Days 29–44). The decline phase was defined as the period when GR was between –10 and –6 (Days 44–48), whereas the death phase was defined as the period when GR was greater than –6 and after the decline phase (Days 48–53). The resulting temporal variation in Chl-*a*

concentrations classified into each period is shown in **Figure 3.5**. In the following sections, atmospheric and seawater parameters are discussed based on these classified growing stages.

### **3.3.2 Temporal variation of DN and DOC in seawater**

**Figure 3.6** shows temporal changes in concentrations of DN and DOC, the DN/DOC ratio, together with those of Chl-*a* concentrations. The average values of the parameters obtained during each phase are presented in **Figure 3.7**. The DN and DOC concentrations showed a simultaneous increase with Chl-*a* concentration during the exponential phase. This simultaneous increase suggests that DN and DOC were released from *Trichodesmium* associated with its increasing numbers and activities, such as primary production and nitrogen fixation. A similar result was obtained by Mulholland et al. [2004], who showed that nitrogen fixation rates increased associated with the growth of *Trichodesmium*, followed by an increase in DON and  $\text{NH}_4^+$  concentration in seawater by a laboratory incubation experiment. DN concentrations continued to increase even during the stationary and decline phases when Chl-*a* concentrations continuously decreased. This may be due to the reduction of the amount of DN consumed/recycled by *Trichodesmium* during the stationary and decline phases. It is also possible that the production of DN was enhanced due to increased decomposition by bacteria. Indeed, this is partly supported by a significant increase in the cell concentrations of bacteria during

these three phases (**Figure 3.6c**).

It is noted that the decrease in DOC concentration was more evident than DN during the death phase. This implies that DOC was more consumed by bacteria and/or decomposed to be emitted into the atmosphere relative to DN during that phase. It should also be noted that the DN/DOC ratio showed a continuous increase from the exponential to death phases. This result clearly showed that DN was more preferentially produced relative to DOC in terms of the net amount from the exponential to death phases. Note that the accumulation of DN and DOC, particularly during the decline and death phases, might contribute to the increase in those concentrations, which was different from the actual condition in the ocean where dynamical mixing and consumption of DN and DOC by other microorganisms occur. Nevertheless, the experimental result showed that DN and DOC were released associated with nitrogen fixation during the exponential and stationary phases.

### **3.3.3 Temporal variation of atmospheric reactive nitrogen**

**Figure 3.8** shows the time series of WSON concentrations in the particle and gas phases, together with the concentrations of seawater parameters throughout the experiment. The average concentrations of each parameter during each growth phase are summarized in **Figures 3.9a** and **3.10a**. The mass concentration of WSON in the particle phase showed an increase during the exponential phase with a maximum value of 34.2

ngN m<sup>-3</sup> (**Figure 3.8a**), while it decreased during the decline and death phases. Concentrations of gas-phase acidic WSON increased during the exponential and stationary phases and decreased during the decline and death phases. This temporal trend is similar to that of Chl-*a*. The result suggests that acidic compounds of DN, which were exudates in nitrogen fixation by *Trichodesmium* in seawater, were emitted into the atmosphere as gas-phase acidic WSON. On the other hand, the gas-phase basic WSON showed extremely high concentrations during the decline and death phases, with averages of 2.5±2.0 µgN m<sup>-3</sup> and 2.7±3.2 µgN m<sup>-3</sup>, respectively. The maximum concentration of gas-phase basic WSON was as high as ~8.0 µgN m<sup>-3</sup> observed during the death phase. Although specific compounds of gas-phase basic WSON were not measured in this study, some semi-volatile WSON compounds, such as alkylamines, are one of the candidates.

**Figure 3.11** shows temporal variations in the NH<sub>4</sub><sup>+</sup> and NH<sub>3</sub> concentrations during the experiment. The average concentrations during each growth phase are also summarized in **Figures 3.9b** and **3.10b**. The concentration of particle-phase NH<sub>4</sub><sup>+</sup> showed an increase during the exponential phase, with its peak during the stationary phase. The concentration of NH<sub>4</sub><sup>+</sup> decreased during the decline and death phases. In contrast, NH<sub>3</sub> concentrations showed extremely high concentrations during the decline and death phases, with a maximum concentration of ~19 µg m<sup>-3</sup>. This temporal trend is similar to that of gas-phase basic WSON. The simultaneous increase in the concentrations of gas-phase basic WSON and NH<sub>3</sub> during the decline and death phases suggest the decomposition of DN and dead

cells of *Trichodesmium* by photochemical reactions and/or bacteria in the culture medium resulted in the increased atmospheric emissions of such basic reactive nitrogen.

**Figure 3.12** shows temporal variations of  $\text{NO}_3^-$  and  $\text{NO}_2^-$  in the particle phase and  $\text{HNO}_3$  and HONO in the gas phase. The average concentrations during each growth phase are summarized in **Figures 3.9c, 3.9d, and 3.10c**. Concentrations of particulate  $\text{NO}_3^-$  showed a slight increase associated with the growth of *Trichodesmium*. The concentrations of gas-phase  $\text{HNO}_3$  and HONO increased during the exponential and stationary phases, while these levels were much lower than those of WSON and  $\text{NH}_4^+/\text{NH}_3$ . The increase in the concentrations of nitrate and nitrite was likely produced by the nitrification of DN in the culture medium, resulting in the formation of gas-phase  $\text{HNO}_3$  and HONO.

### **3.3.4 Gas-particle phase partitioning and budget of reactive nitrogen species associated with the growth of *Trichodesmium***

**Figure 3.13** shows the mass fraction of particle-, acidic gas-, and basic gas-phases of each reactive nitrogen species in each growth phase. For WSON, the mass fraction of gas-phase basic WSON increased from stationary to death phases. For  $\text{NH}_4^+/\text{NH}_3$ , gas-phase ( $\text{NH}_3$ ) dominated during the entire period. With regard to  $\text{NO}_3^-/\text{HNO}_3$ , the fraction of particle phase increased as the growth stage proceeded, the trend of which was similar to that of  $\text{NO}_2^-/\text{HONO}$ . Since  $\text{NH}_3$  and basic WSON are neutralizing agents of  $\text{HNO}_3$  to

form particles (e.g.,  $\text{NH}_4\text{NO}_3$ ), this trend was explained by gas-to-particle shift/formation of nitrate and nitrite due to the increase in the emission of  $\text{NH}_3$  and basic WSON from the stationary to death phases.

**Figure 3.14** shows the mass fraction of each reactive nitrogen species in the particle and gas phases. In the particle phase,  $\text{NH}_4^+$  was the most dominant component, which accounted for 62% of the total reactive nitrogen, followed by WSON (33%) throughout the growth stage of *Trichodesmium*. In the acidic gas phase, WSON was the most dominant reactive nitrogen, which accounted for 68% on average. In the basic gas phase,  $\text{NH}_3$  was the most dominant (89%), followed by WSON. **Figure 3.15** shows the mass fraction of each gas-phase reactive nitrogen to the total. As is expected from **Figure 3.14**,  $\text{NH}_3$  was the most dominant component (86%), whereas the mass fraction of gas-phase basic WSON increased during the decline and death phases. This means that the relative contribution of sea-to-air emissions of gas-phase basic WSON became larger during those phases.

### **3.3.5 Nitrogen-to-carbon ratios of the parameters in the atmospheric and seawater samples**

In this section, N/C ratios of atmospheric and seawater parameters are discussed. **Figure 3.16** shows the time series of WSOC concentrations in the particle and gas phases, together with the concentrations of seawater parameters throughout the experiment. In

general, mass concentrations of both acidic and basic WSOC in the gas phase increased during the exponential and stationary phases and decreased during the decline and death phases. This temporal trend is similar to that of DOC and Chl-*a* concentration. The result suggests that acidic and basic compounds of DOC, which were also like exudates by nitrogen fixation by *Trichodesmium* in seawater, were emitted into the atmosphere as gas- and particle-phase WSOC.

**Figure 3.17** shows the average values of the WSTN/WSOC ratio (the sum of the total mass of particle and gas phases) in the atmospheric samples and DN/DOC ratio in the seawater samples in each growth phase. For reference, the C/N ratios of those data are shown in **Table 3.2**. Throughout the experiment, the N/C ratios in the atmospheric samples were larger than those in the seawater samples. Specifically, the N/C ratios in the atmospheric samples during the exponential and stationary phases (both 0.83) were 6-12 times higher than those in seawater (0.07 and 0.13 during the exponential and stationary phases, respectively). These results suggest preferential sea-to-air emissions of reactive nitrogen relative to organic carbon associated with the growth of *Trichodesmium*. This may be due to more volatile characteristics of DN relative to DOC released by *Trichodesmium* as well as the following decomposition of those components. During the decline and death phases, the WSTN/WSOC ratios in the atmosphere increased significantly relative to the increase in the DN/DOC ratio in seawater. This result suggests the consumption of DOC by bacteria and decomposition of DN and dead cells of



*Trichodesmium* by photochemical reactions and/or bacteria followed by sea-to-air emissions of DN relative to those of DOC during those phases.

### 3.3.6 Sea-to-air emission flux of reactive nitrogen

To quantitatively evaluate atmospheric reactive nitrogen produced associated with the growth of *Trichodesmium*, the sea-to-air emission flux of WSTN ( $F_{WSTN}$ ) was calculated using the following equation:

$$F_{WSTN} = \frac{(C - C_b) \times V}{S \times \Delta t}$$

where  $C$  denotes the concentration of WSTN ( $\text{ngN m}^{-3}$ ),  $C_b$  denotes the background concentration of WSTN ( $\text{ngN m}^{-3}$ ) in the experimental system,  $V$  denotes sampled air volume ( $\text{m}^3$ ),  $S$  denotes the area of sea surface ( $\text{m}^2$ ) of the experimental tank, and  $\Delta t$  denotes sampling duration (day). It should be noted that the experimental conditions of this system differ from those of the actual ocean-atmospheric environment. Hence, the following ambient conditions are assumed in this calculation: low atmospheric pressure, low wind speed with no waves, and active cyanobacterial bloom at the ocean surface.

**Figure 3.18** shows the average sea-to-air flux of the total WSTN in each growth phase of *Trichodesmium* during the experiment. The fluxes during the decline and death phases were substantially higher than those during the exponential and stationary phases, which

reflected the significant difference in the mass concentration of WSTN in the two periods. The average flux was  $2.9 \pm 2.7$  ( $\text{mgN m}^{-2} \text{ day}^{-1}$ ), which is substantially larger than the  $\text{NH}_4^+$  flux ( $0.06\text{--}0.27 \text{ mgN m}^{-2} \text{ day}^{-1}$ ) estimated for the subtropical North Pacific by global biogeochemical model [Poulot et al., 2015]. Because the difference in the estimated flux may be partly due to the extremely high concentrations of Chl-*a* (i.e., the amount of *Trichodesmium*) in the current experimental system, the flux per unit mass of Chl-*a* was calculated for direct comparison. (**Table 3.3**). The result showed that the flux during the stationary phase estimated in this study accounted for only  $\sim 1\%$  of that estimated by Poulot et al. [2015], whereas the flux during the decline phase accounted for up to  $\sim 40\%$  of the flux estimated for the subtropical North Pacific. Despite the uncertainty in the flux calculation and experimental conditions, the result suggests that DN released associated with nitrogen fixation can partly explain sea-to-air emissions of water-soluble nitrogen, including WSON and ammonia.

### 3.4 Conclusion

To investigate the contribution of nitrogen-fixing organisms to the formation of atmospheric reactive nitrogen, the non-heterocystous, diazotrophic cyanobacterium *Trichodesmium erythraeum* (CCMP1985), as a representative nitrogen-fixing organism, was incubated in artificial seawater under controlled light and temperature in a laboratory. Simultaneously, continuous atmospheric sampling of particulate and gas-phase reactive

nitrogen was conducted with discrete seawater collection over 55 days. The concentrations of DN and DOC in seawater showed a simultaneous increase with Chl-*a* concentration during the exponential phase, suggesting that DN and DOC were released by *Trichodesmium* associated with its nitrogen fixation. DN concentrations continued to increase even from the stationary phase to the death phase, which was likely due to a reduction in the amount of DN consumed or recycled by *Trichodesmium* during those phases. Furthermore, the continuous increase of the DN/DOC ratio throughout the experiment indicates larger net production of DN relative to that of DOC in seawater during the growth and decline phases of *Trichodesmium*.

$\text{NH}_4^+/\text{NH}_3$  was the most abundant reactive nitrogen species, followed by WSON in the particle and gas phases throughout the entire period. On average,  $\text{NH}_4^+$  and WSON accounted for 62% and 33% of the reactive nitrogen species, respectively, measured in the particle phase. Meanwhile, in the gas phase,  $\text{NH}_3$  and WSON accounted for 86% and 13% of the reactive nitrogen, respectively. In particular, basic WSON was found to be the second most abundant reactive nitrogen species.  $\text{NH}_4^+$ , particle-phase WSON, and gas-phase acidic WSON showed increased concentrations during the exponential and stationary phases. On the other hand, it was found for the first time that concentrations of  $\text{NH}_3$  and basic WSON in the gas phase showed a significant increase during the decline and death phases of *Trichodesmium*. The substantial increase in the atmospheric emissions of  $\text{NH}_3$  and basic WSON was likely due to the considerable decomposition of

DN by bacteria and/or photochemical reactions in seawater during those phases. This is followed by producing low-molecular-weight, more volatile, basic DN that was more easily transferred from seawater to the atmosphere.

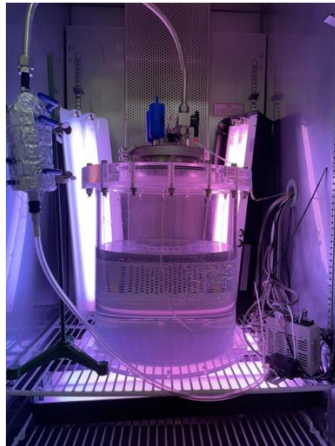
The overall experiments demonstrated sea-to-air emissions of  $\text{NH}_4^+/\text{NH}_3$  and WSON associated with the growth and decline of *Trichodesmium*. Furthermore, the results suggested that gas-phase organic nitrogen mainly consisted of highly volatile, basic components whose emission significantly increased with an increase in heterotrophic bacteria during the decline and death phases of *Trichodesmium*. Our results suggest, for the first time, that the source of ammonia/ammonium and WSON associated with nitrogen fixation are crucial for changing atmospheric acidity and particle formation over the ocean, as they all have the nature of alkalinity in the atmosphere.

## References

- Bernard, F., Ciuraru, R., Boréave, A. & George, C. Photosensitized formation of secondary organic aerosols above the air/water interface. *Environ. Sci. Technol.* 50, 8678–8686, 2016.
- Boatman, T. G., Lawson, T., and Geider, R. J.: A key marine diazotroph in a changing ocean: The interacting effects of temperature, CO<sub>2</sub> and light on the growth of *Trichodesmium erythraeum* IMS101, *PLOS ONE*, 12, e0168796, <https://doi.org/10.1371/journal.pone.0168796>, 2017.
- Chen Y. B., Zehr J. P., Mellon M.: Growth and nitrogen fixation of the diazotrophic filamentous nonheterocystous cyanobacterium *Trichodesmium* sp. IMS101 in defined media: evidence for a circadian rhythm, *J. Phycol.*, 32, 916–923, 10.1111/j.0022-3646.1996.00916.x, 1996.
- Drugé, T., Nabat, P., Mallet, M., and Somot, S.: Model simulation of ammonium and nitrate aerosols distribution in the Euro-Mediterranean region and their radiative and climatic effects over 1979–2016, *Atmos. Chem. Phys.*, 19, 3707–3731, <https://doi.org/10.5194/acp-19-3707-2019>, 2019.
- Hauglustaine, D. A., Balkanski, Y., and Schulz, M.: A global model simulation of present and future nitrate aerosols and their direct radiative forcing of climate, *Atmos. Chem. Phys.*, 14, 11031–11063, <https://doi.org/10.5194/acp-14-11031-2014>, 2014.
- Mahaffey, C., Michaels, and AF., Capone, DG.: The conundrum of marine Nitrogen fixation, *Am J Sci*, 305:546–595, (2005).
- Mulholland MR, Bronk DA, Capone DG.: Dinitrogen fixation and release of ammonium and dissolved organic nitrogen by *Trichodesmium* IMS 101, *Aquat Microb Ecol.*, 37:85–94, 2004.
- Paulot, F., Crounse, J. D., Kjaergaard, H. G., Kroll, J. H., Seinfeld, J. H., and Wennberg, P. O.: Isoprene photooxidation: new insights into the production of acids and organic nitrates, *Atmos. Chem. Phys.*, 9, 1479–1501, doi:10.5194/acp-9-1479-2009, 2009.
- Paulot, F., Jacob, D. J., Johnson, M. T., Bell, T. G., Baker, A. R., Keene, W. C., Lima, I. D., Doney, S. C., and Stock, C. A.: Global oceanic emission of ammonia:

- Constraints from seawater and atmospheric observations, *Global Biogeochem. Cycles*, 29, 1165–1178, <https://doi.org/10.1002/2015GB005106>, 2015.
- Rastelli, E., Corinaldesi, C., Dell’Anno, A., Martire, M. L., Greco, S., Facchini, M. C., et al.: Transfer of labile organic matter and microbes from the ocean surface to the marine aerosol: An experimental approach. *Scientific Reports*, 7(1), 1–10. <https://doi.org/10.1038/s41598-017-10563-z>, 2017.
- Roberts, J. M.: PAN and Related Compounds, in: *Volatile Organic Compounds in the Atmosphere*, edited by: Koppmann, R., Blackwell Publishing, 500, Oxford, UK, 2007.
- Suzuki, K., A. Kamimura, and S. B. Hooker.: Rapid and highly sensitive analysis of chlorophylls and carotenoids from marine phytoplankton using ultra-high performance liquid chromatography (UHPLC) with the first derivative spectrum chromatogram (FDSC) technique, *Mar. Chem.*, 176, 96–109, [doi:10.1016/j.marchem.2015.07.010](https://doi.org/10.1016/j.marchem.2015.07.010), 2015.
- Westberry, TK., and Siegel, DA.: Spatial and temporal distribution of Trichodesmium blooms in the world's oceans, *Global Biogeochem Cycles*, 20:GB4016, [doi: 10.1029/2005GB002673](https://doi.org/10.1029/2005GB002673), 2006.
- Yu, Z.; Li, Y. Marine volatile organic compounds and their impacts on marine aerosol—A review. *Sci. Total Environ.*, 768, 145054, 2021.
- Zehr, J. P. and Capone, D. G.: Changing Perspectives in Marine Nitrogen Fixation, *Science*, 368, eaay9514, [doi: 10.1126/science.aay9514](https://doi.org/10.1126/science.aay9514), 2020.

(a)



(b)

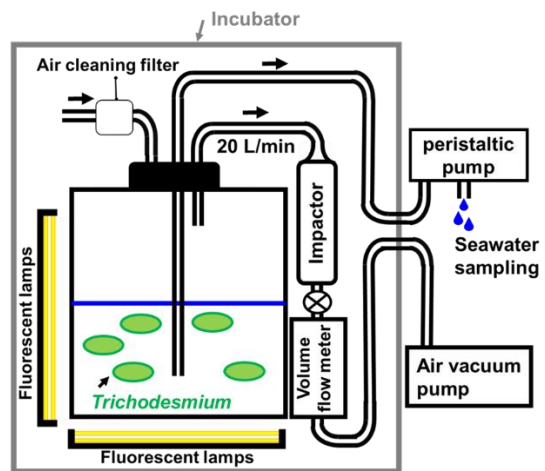


**Figure 3.1** An experimental system setup for the incubation of *Trichodesmium* in artificial seawater and collection of atmospheric and seawater samples ((a) picture and (b) schematic diagram of the system).

(a)



C (coarse particle)  
:  $D_p > 2.5 \mu\text{m}$

P (particle)  
:  $D_p < 2.5 \mu\text{m}$

G<sub>1</sub>(gas)  
: for acidic gas

G<sub>2</sub> (gas)  
: for basic gas

(b)



C :  $D_p > 2.5 \mu\text{m}$ , Quartz fiber filters  
 P :  $D_p < 2.5 \mu\text{m}$ , Quartz fiber filters  
 G<sub>1</sub> : Acidic gas, 2%Na<sub>2</sub>CO<sub>3</sub> impregnated cellulose filter  
 G<sub>2</sub> : Basic gas, 2%H<sub>3</sub>PO<sub>4</sub> impregnated cellulose filter

**Figure 3.2** NILU impactor for collection of atmospheric particle and gas-phase samples.

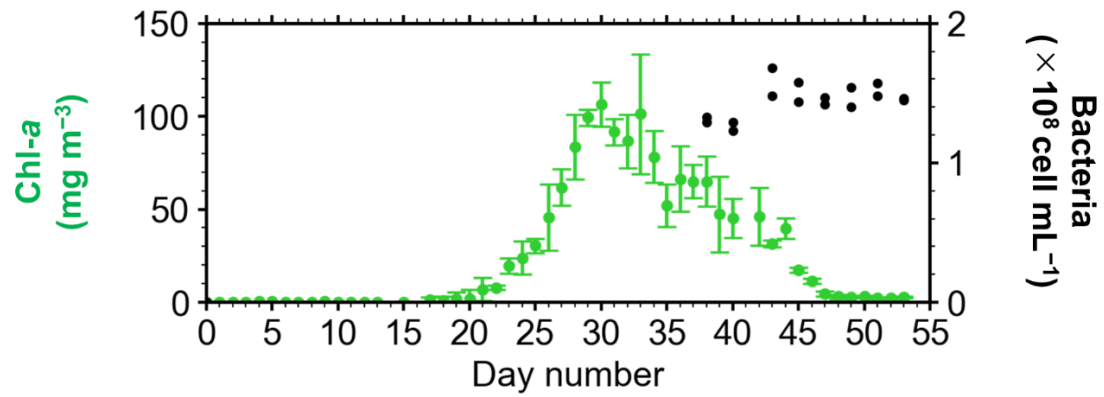


**Figure 3.3** Temporal variations in the concentrations of Chl-*a* associated with the incubation of *Trichodesmium* and bacteria in artificial seawater.

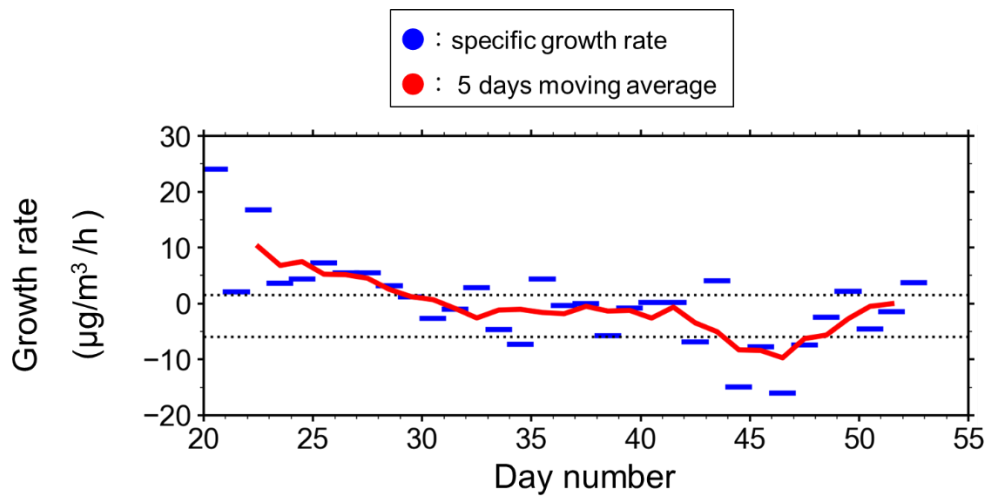


**Figure 3.4** Temporal variation of the growth rate of *Trichodesmium* for individual seawater samples together with 5-day running-mean values.



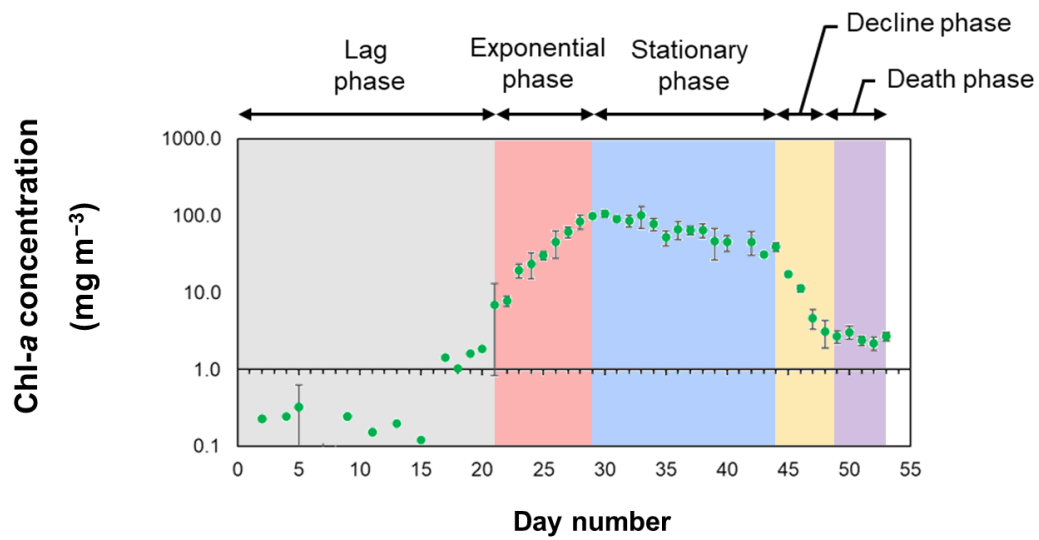


**Figure 3.5** A schematic of each growth phase of *Trichodesmium* defined by its growth rate, together with the temporal variation of Chl-*a* concentration.

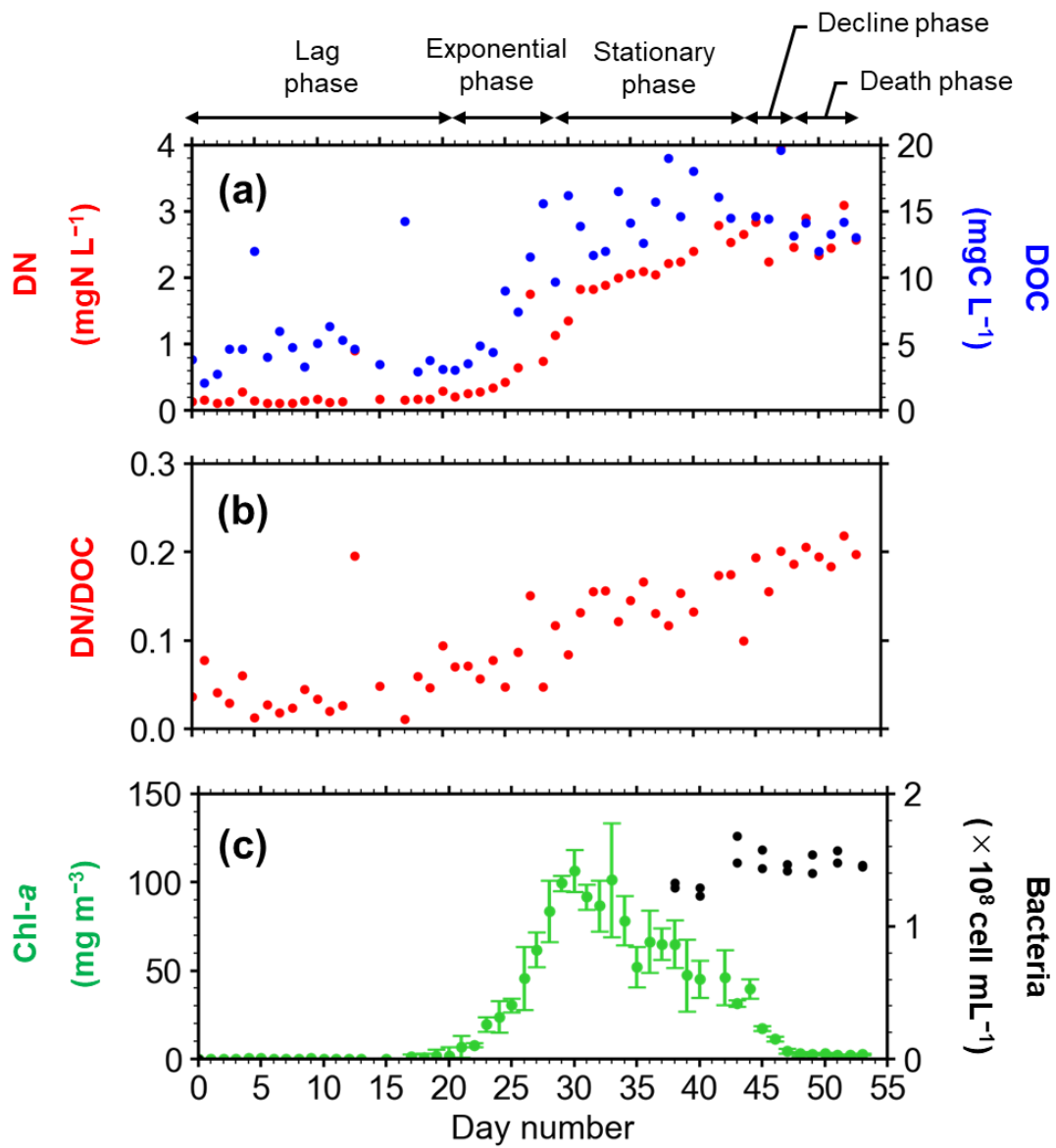


**Figure 3.6** Temporal variation in (a) DN and DOC concentrations, (b) DN/DOC ratios, and (c) Chl-*a* and bacteria concentrations in artificial seawater during the experiment.

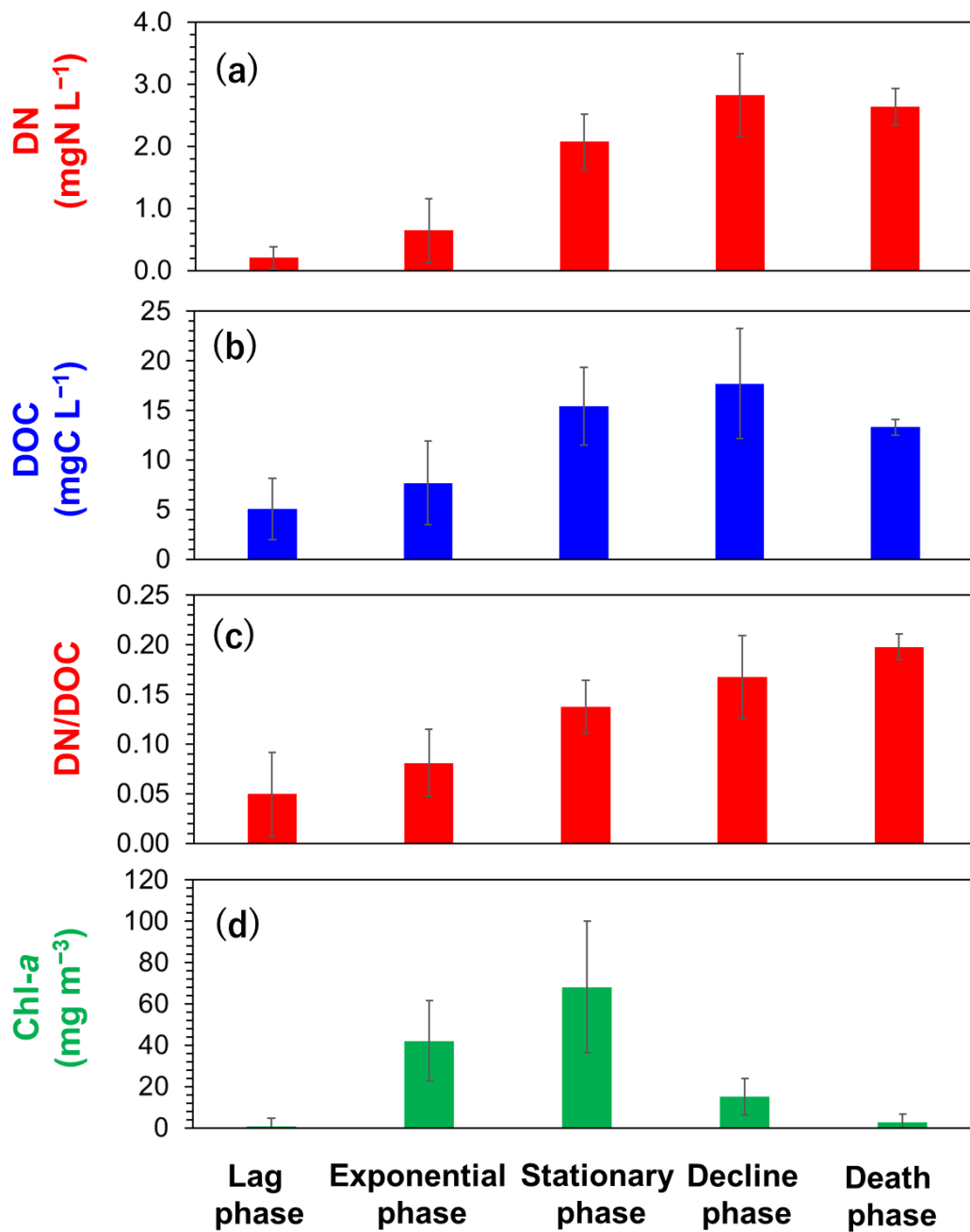


**Figure 3.7** Average concentrations of (a) DN, (b) DOC, (c) DN/DOC, and (d) Chl-*a* during each growth phase of *Trichodesmium*.

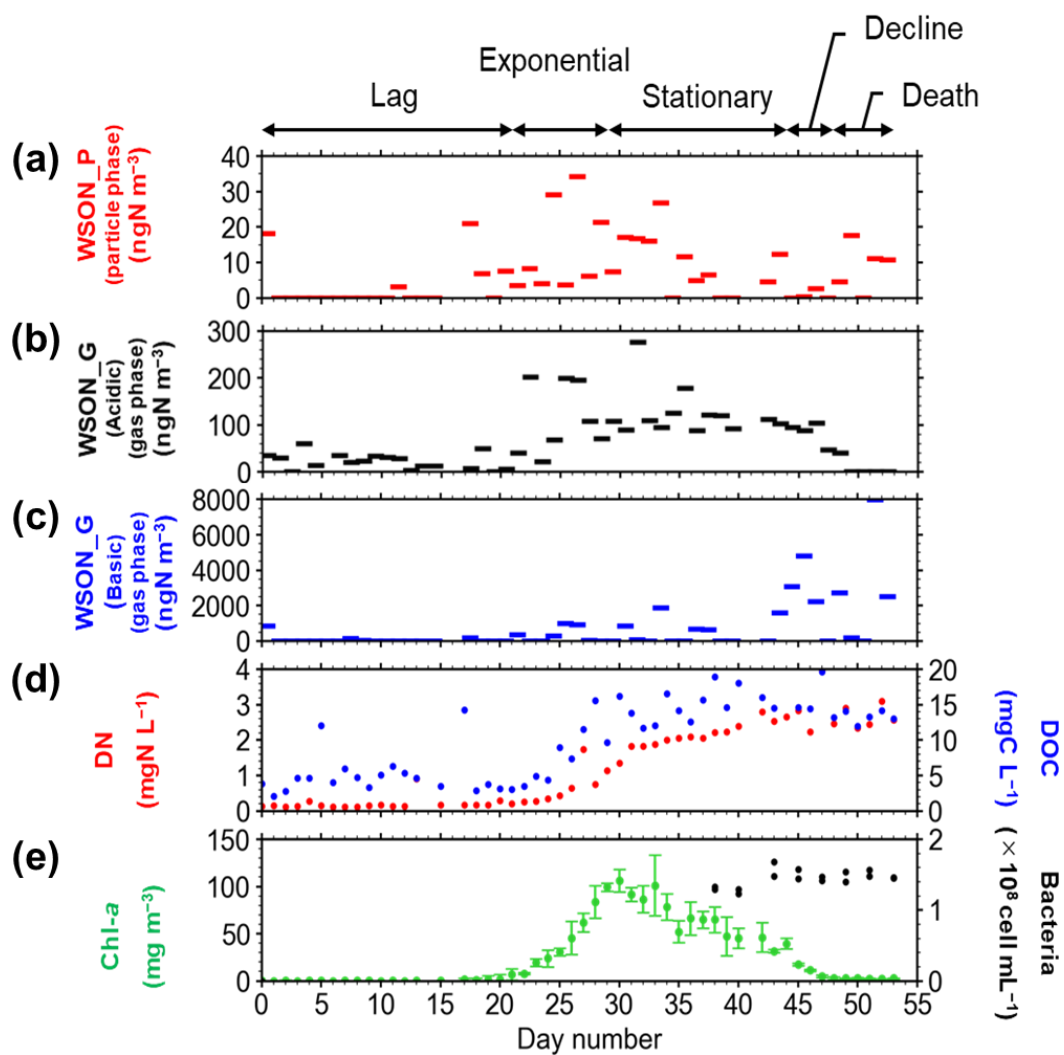


**Figure 3.8** Temporal variation in the concentrations of (a) WSON (particle phase), (b) WSON (acidic gas phase), (c) WSON (basic gas phase) in atmospheric samples, and concentrations of (d) DN and DOC, and (e) Chl-a and bacteria in seawater samples.

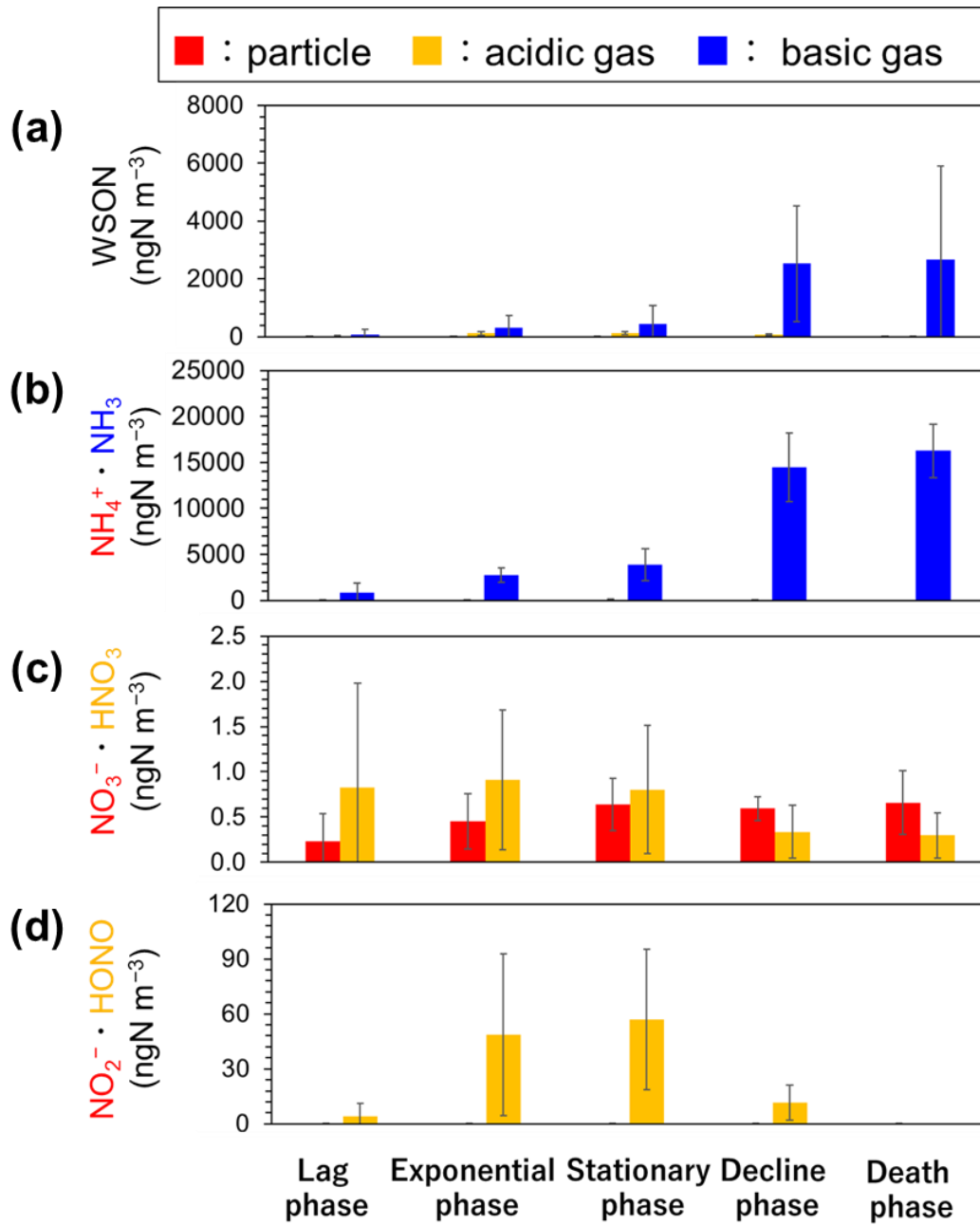


**Figure 3.9** Average concentrations of (a) WSON, (b)  $\text{NH}_4^+$ ,  $\text{NH}_3$ , (c)  $\text{NO}_3^-$ ,  $\text{HNO}_3$ , (d)  $\text{NO}_2^-$ , and  $\text{HONO}$  in each growth phase of *Trichodesmium*.

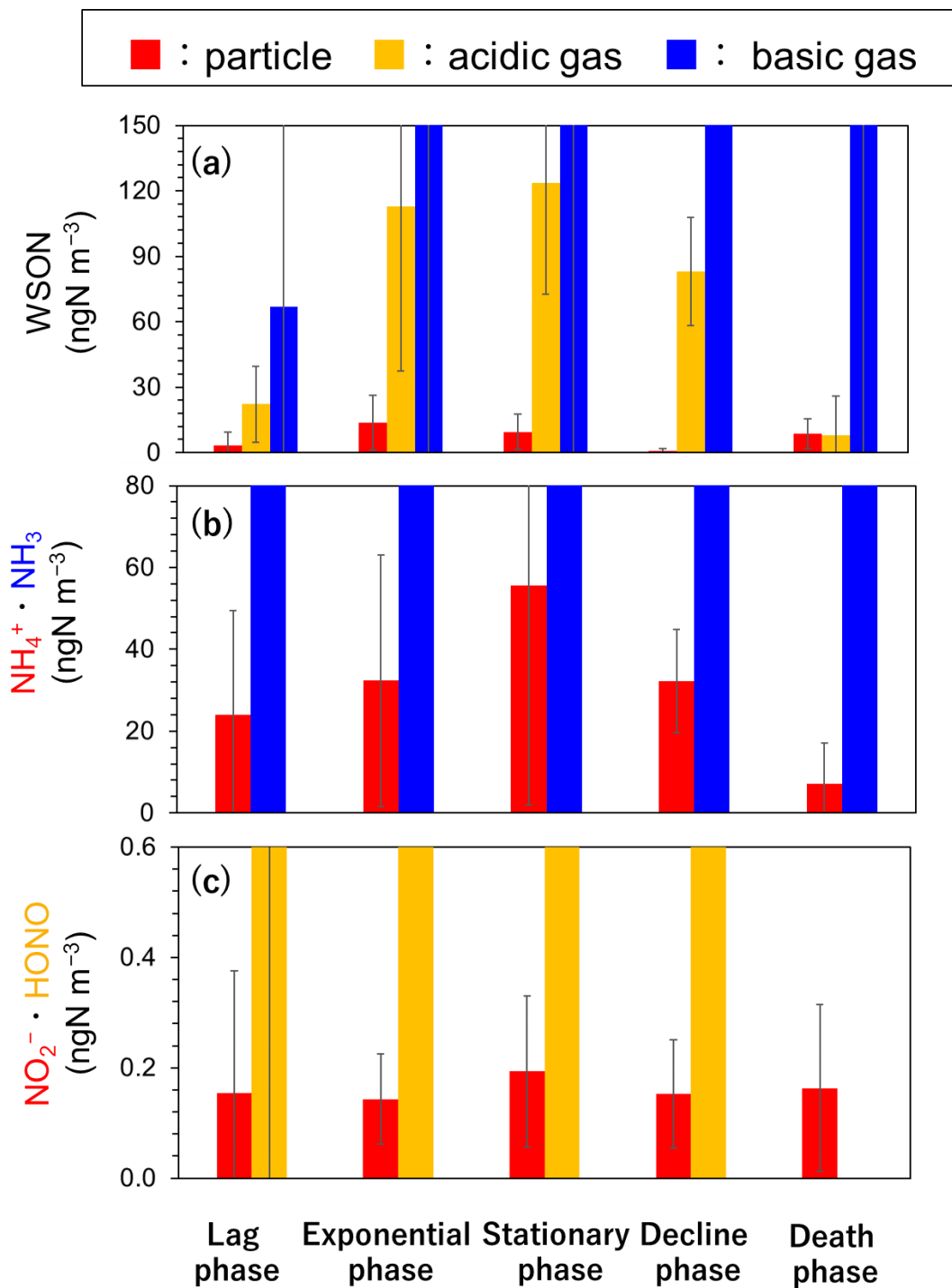


**Figure 3.10** Same as Figure 3.9 except for NO<sub>3</sub><sup>-</sup> and HNO<sub>3</sub>. The scales of the y-axis are different from those in Figure 3.9.

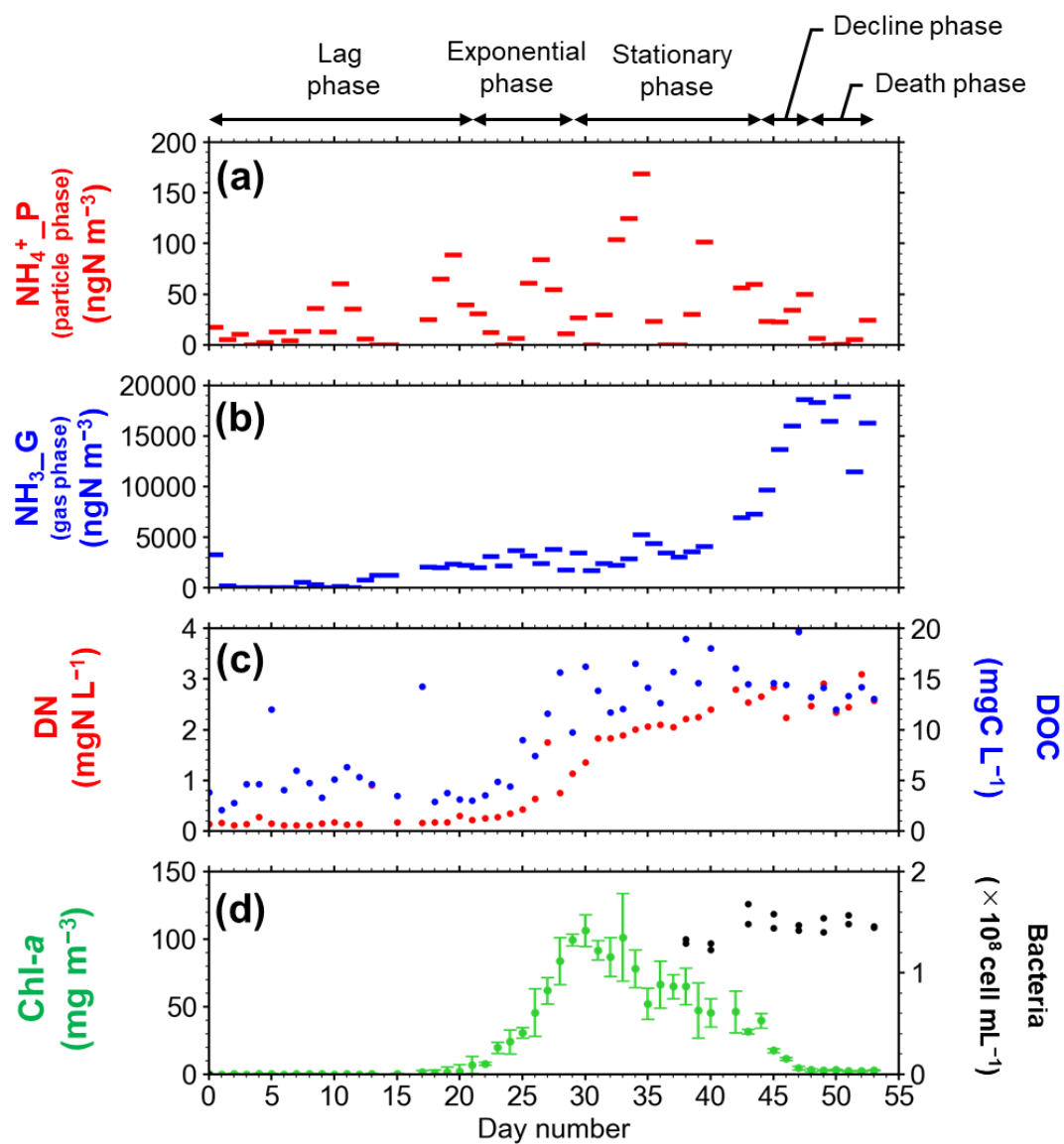


**Figure 3.11** Temporal variation of atmospheric concentrations of (a)  $\text{NH}_4^+$  (particle phase) and (b)  $\text{NH}_3$  (gas phase), and seawater concentrations of (c) DN, DOC, (d) Chl-*a*, and bacteria.

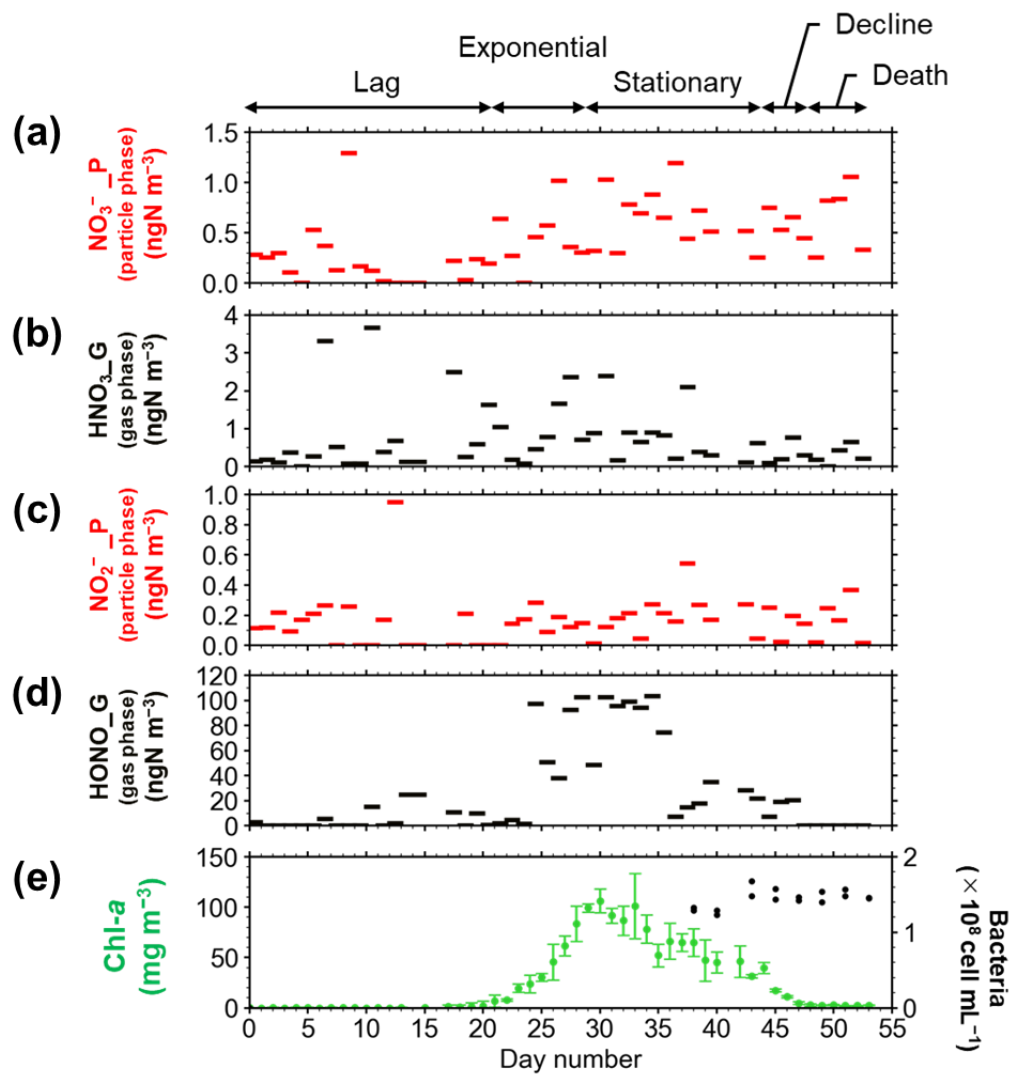


**Figure 3.12** Temporal variation of (a)  $\text{NO}_3^-$  (particle phase), (b)  $\text{HNO}_3$  (gas phase), (c)  $\text{NO}_2^-$  (particle phase), (d)  $\text{HONO}$  (gas phase), and (e)  $\text{Chl-a}$  and bacteria.



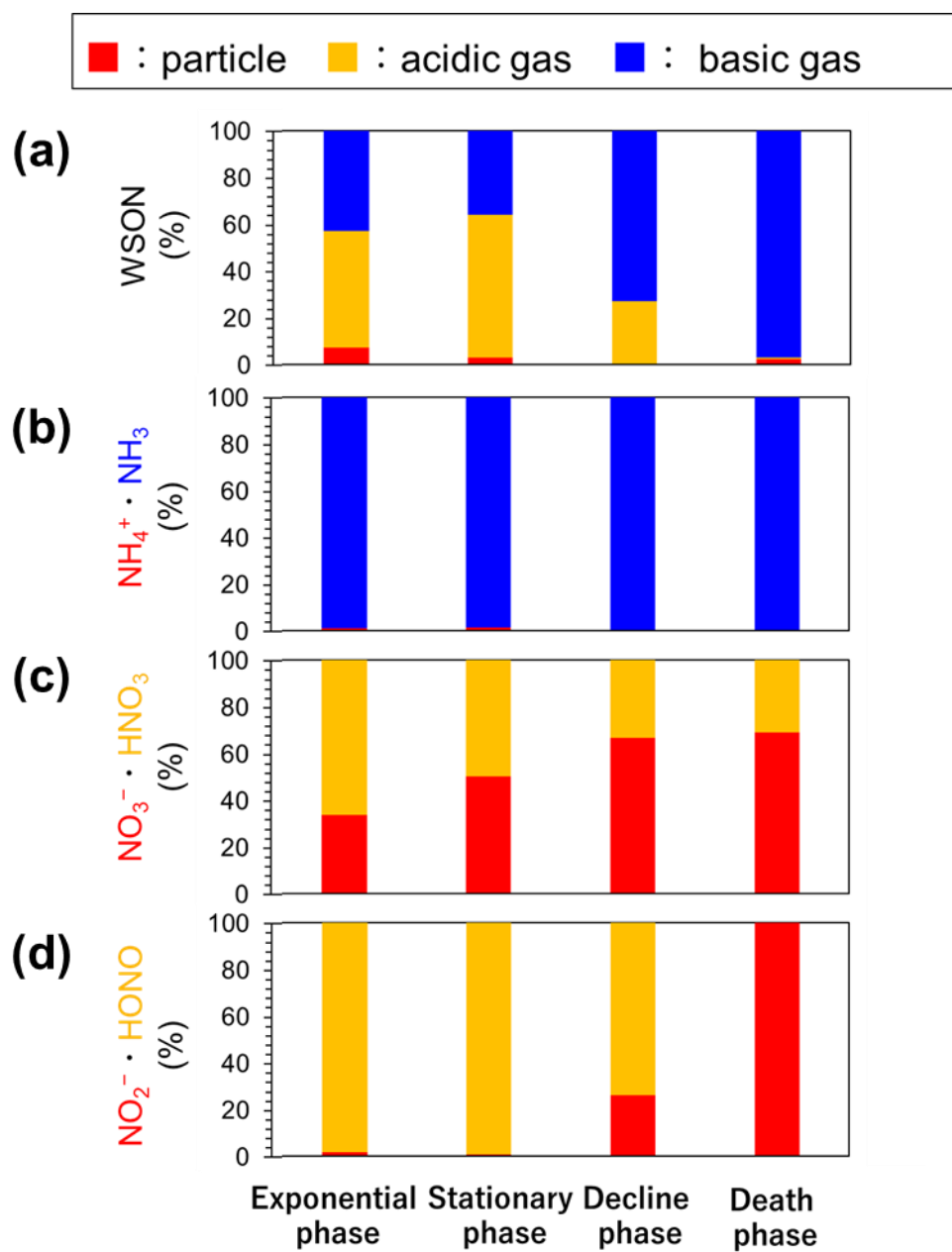


**Figure 3.13** Average mass fractions of particle and gas phases of (a) WSON, (b)  $\text{NH}_4^+/\text{NH}_3$ , (c)  $\text{NO}_3^-/\text{HNO}_3$ , (d)  $\text{NO}_2^-/\text{HONO}$  in each growth phase of *Trichodesmium*.

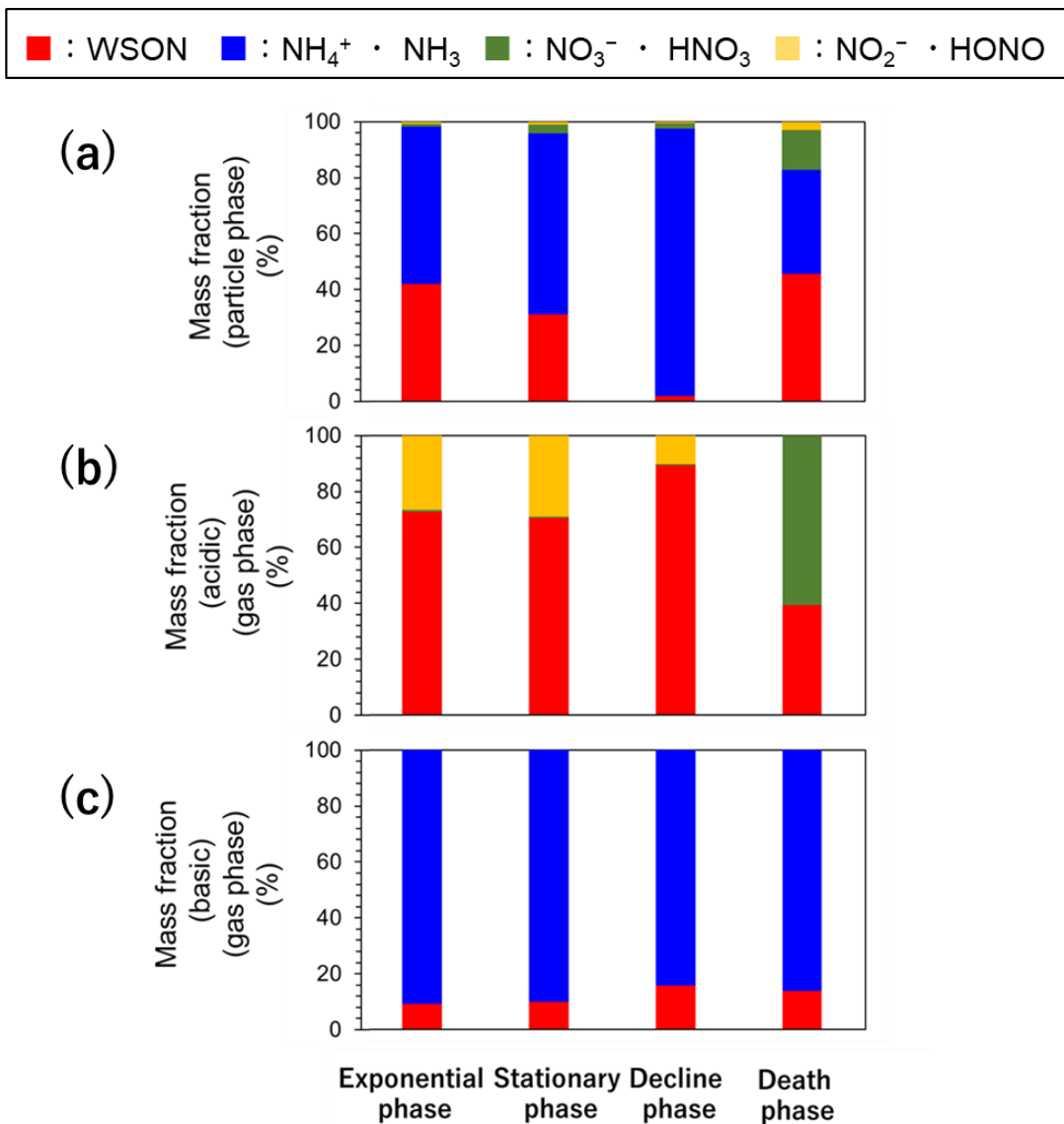


**Figure 3.14** The average chemical mass fractions of reactive nitrogen species in the (a) particle phase, (b) acidic gas phase, and (c) basic gas phase in each growth phase of *Trichodesmium*.

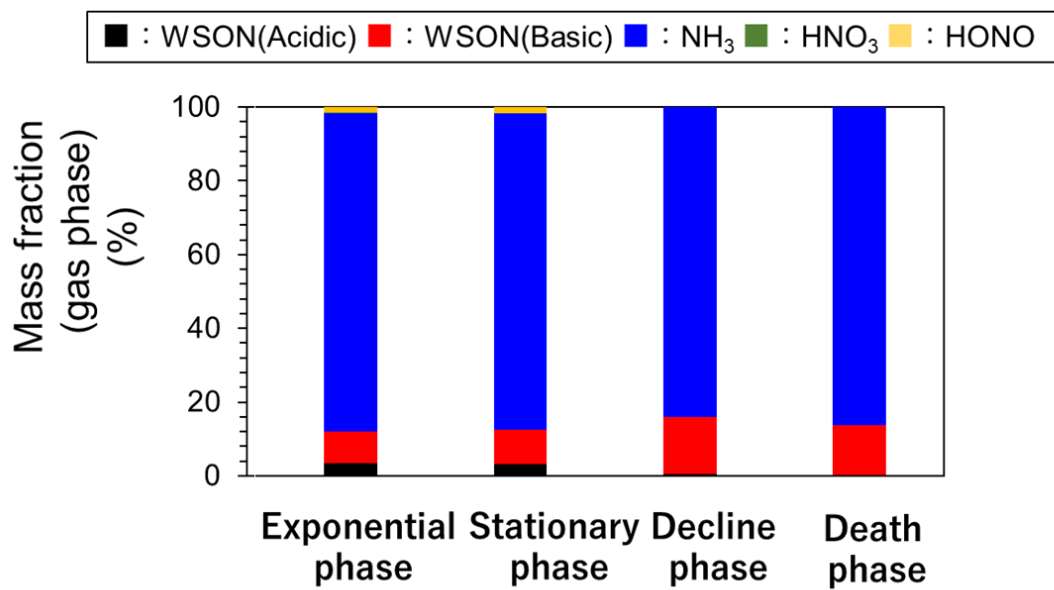


**Figure 3.15** The average chemical mass fractions of reactive nitrogen species in the gas phase in each growth phase of *Trichodesmium*.

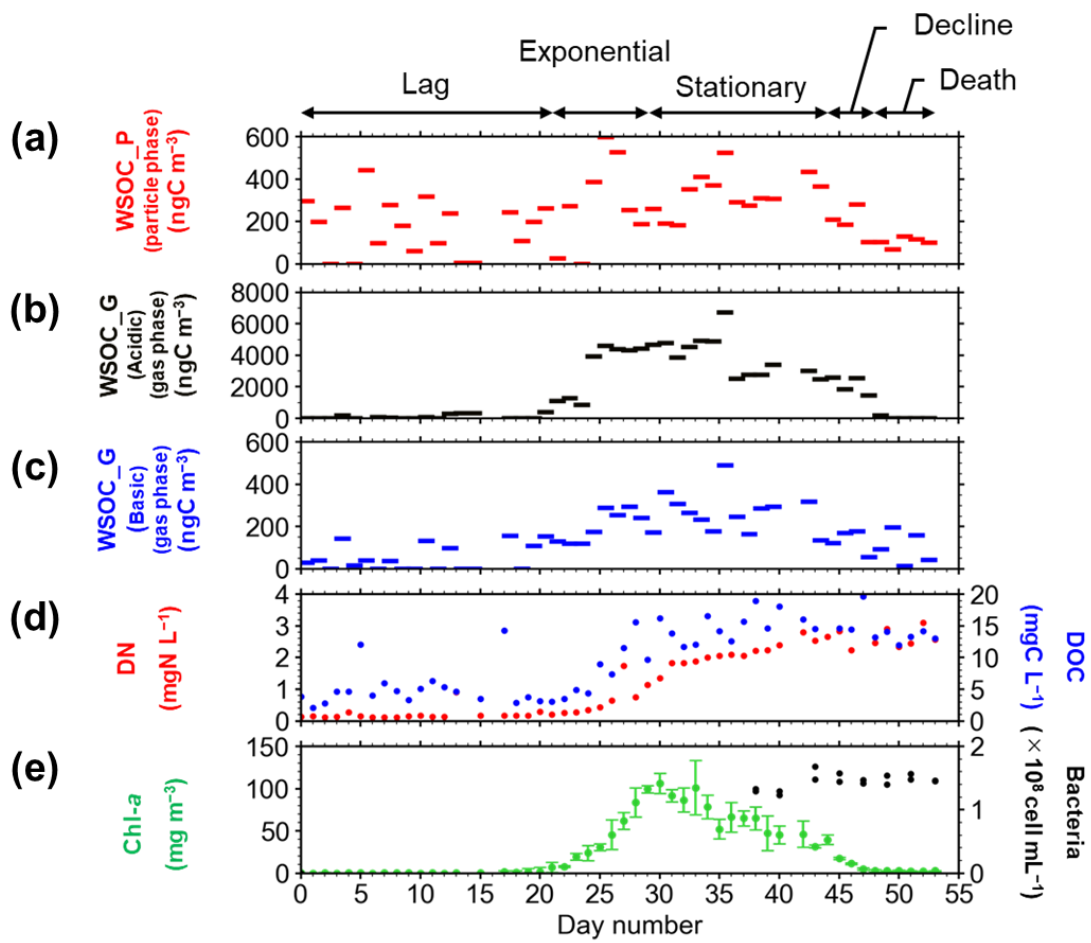


**Figure 3.16** Temporal variation of concentrations of WSOC in (a) the particle phase, (b) the acidic gas phase, and (c) the basic gas phase. Also shown are concentrations of (d) DN, DOC, (e) Chl-*a* and bacteria in seawater.

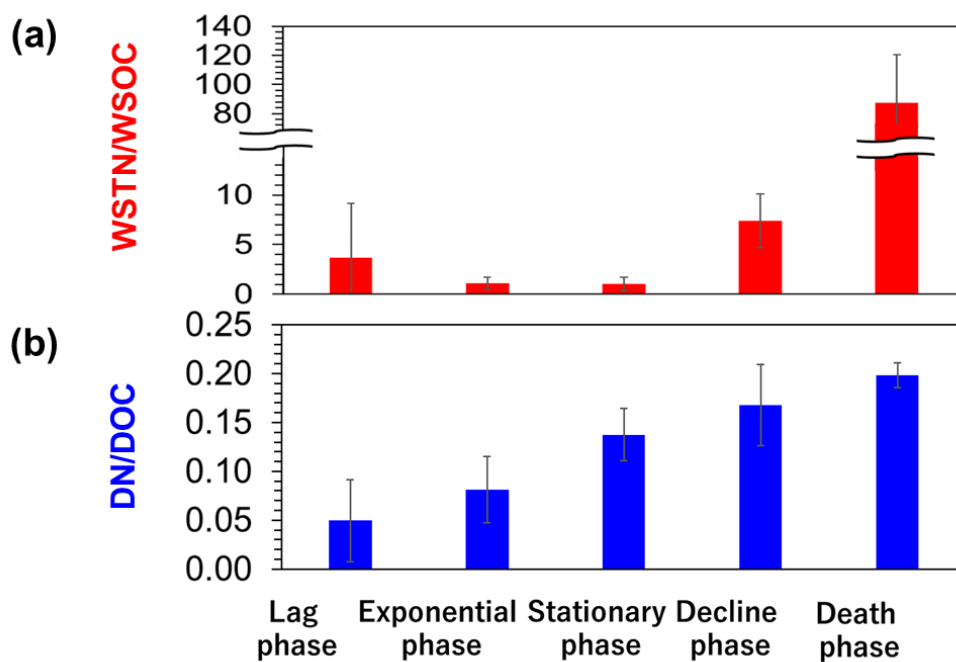


**Figure 3.17** Average values of (a)  $WSTN/WSOC$  in the atmospheric samples and (b)  $DN/DOC$  in the seawater in each growth phase.

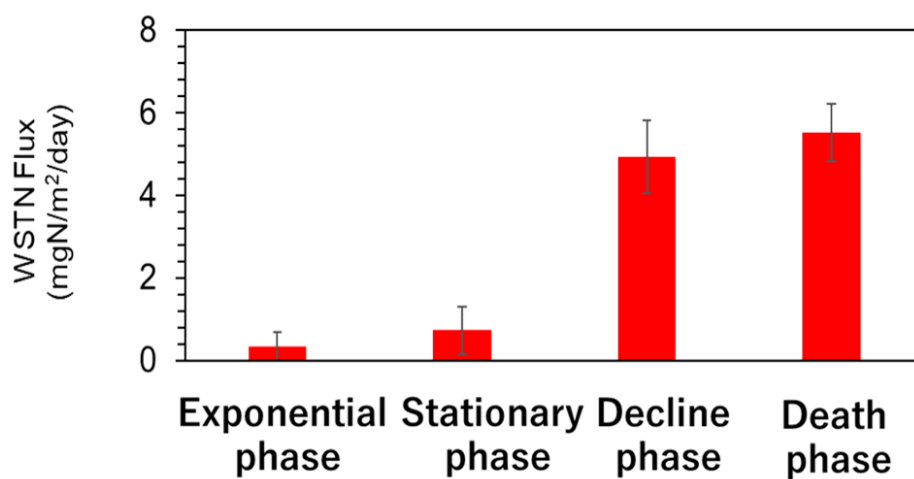


**Figure 3.18** Average values of the sea-to-air flux of  $WSTN$  in each growth phase.

**Table. 3.1** Each growth stage defined by 5-day running-mean values of the growth rate (GR;  $\mu\text{g m}^{-3} \text{h}^{-1}$ ) of *Trichodesmium*.

Growth stage	GR range	day number
Lag phase	--- ( $[\text{Chl-}a] < 2.0 \text{ mg m}^{-3}$ )	0–21
Exponential phase	$1.5 \leq \text{GR}$	21–29
Stationary phase	$-6 \leq \text{GR} \leq 1.5$	29–44
Decline phase	$-10 \leq \text{GR} \leq -6$	44–48
Death phase	$-6 \leq \text{GR}$	48–53

**Table. 3.2** C/N ratio in the atmospheric and seawater samples.

	Lag	Exponential	Stationary	Decline	Death
<b>WSOC</b> <b>/WSTN</b>	2.1±3.0	1.2±0.8	1.2±0.5	0.2±0.1	$1.2 \times 10^{-2} \pm 0.4 \times 10^{-2}$
<b>DOC/DN</b>	32.4±22. 3	14.1±5.0	7.6±1.7	6.4±2.1	5.1±0.3

**Table. 3.3** Sea-to-air emission flux of WSTN per Chl-*a* mass.

		Sea-to-air flux ( $\mu\text{gN/m}^2/\text{day}/[\text{Chl-}a \text{ (mg/m}^3)]$ )
<b>Exponential and</b> <b>Stationary phases</b>	<b>This study</b>	<b>7.68 ~10.7</b>
<b>Decline phase</b>	<b>This study</b>	<b>~330</b>
<b>NH<sub>3</sub>/NH<sub>4</sub><sup>+</sup> in the</b> <b>subtropical</b> <b>North Pacific</b>	<b>Paulot et al. (2015)</b>	<b>770–3,830</b>



## Chapter 4. General Conclusions

This study investigated the role of marine nitrogen-fixing organisms in the formation of atmospheric reactive nitrogen based on ship-board observations and laboratory incubation experiments. The ship-board observations were conducted in the oligotrophic subtropical North Pacific from August to October 2017 with simultaneous collection of atmospheric aerosol and surface seawater samples to elucidate the origin of WSON in marine atmospheric aerosols. The average concentration of WSON in fine-mode aerosols along 23°N in the eastern North Pacific ( $7.5 \pm 6.6 \text{ ngN m}^{-3}$ ) was substantially higher than that in the western North Pacific ( $2.4 \pm 1.9 \text{ ngN m}^{-3}$ ) during the research cruise.

The stable carbon isotope ratio of WSOC, together with backward trajectories, indicated that most of the observed WSON in the fine particles in the eastern North Pacific originated from the ocean surface. Relations of the concentrations of WSON with several tracers imply that secondary formation, which differed from the oxidation processes of DMS, was likely the dominant process underlying the formation of WSON observed in this study. Instead, significant positive correlations were found among nitrogen fixation rate, DON concentrations in SSW, and aerosol WSON concentrations. Meanwhile, the undetectable concentrations of EC in aerosols suggest that effects of anthropogenic sources on the observed aerosols were likely small in this study. The overall results suggest that reactive nitrogen (i.e., dissolved organic nitrogen and ammonium) produced



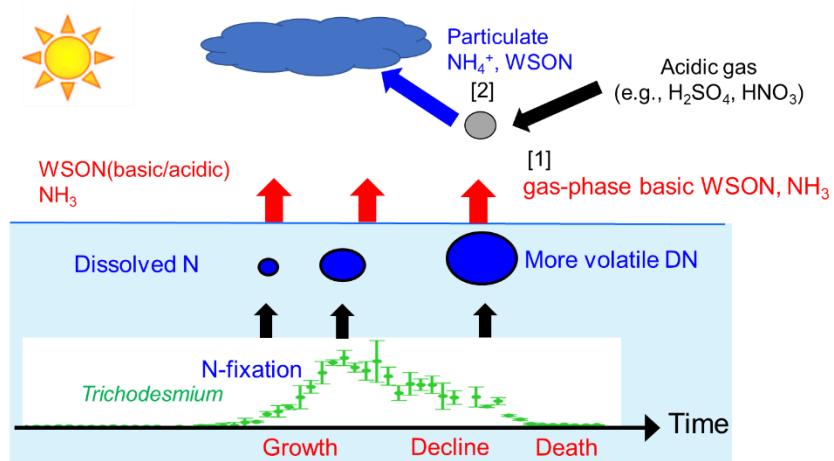
and exuded by nitrogen-fixing microorganisms in SSW likely contributed to the formation of WSON aerosols over the oceanic region.

To prove that reactive nitrogen is emitted into the atmosphere associated with nitrogen fixation, an incubation experiment with simultaneous samplings of atmospheric reactive nitrogen and biological/chemical parameters of artificial seawater was conducted in a laboratory. In the experiment, *Trichodesmium erythraeum* IMS101 was used as representative species of nitrogen-fixing organisms. During the incubation period of two months, the growth and decline phases of the nitrogen-fixing cyanobacterium were observed. During the exponential phase, DN and DOC concentrations in the seawater increased with an increase in Chl-*a* concentrations, suggesting that DN and DOC were released by nitrogen fixation during the growth of *Trichodesmium*.

Throughout the entire period of the experiment, ammonium (62%)/ammonia (86%) were the dominant reactive nitrogen both in particle and gas phases, followed by WSON (particle phase: 33%, gas phase: 13%). A substantial increase in the atmospheric emissions of NH<sub>3</sub> and gas-phase basic WSON was found during the decline and death phases. This result suggests the significant decomposition of DN and dead bacteria cells and/or photochemical reactions in seawater, followed by the production of low-molecular-weight, more volatile, basic DN that were more easily transferred from seawater to the atmosphere. Atmospheric emissions of acidic WSON were larger during the exponential and stationary growth phases of *Trichodesmium*. In contrast, the

emissions of basic reactive nitrogen were more evident during the decline and death phases. The overall results demonstrated sea-to-air emissions of WSON and ammonium/ammonia associated with the growth and decline of *Trichodesmium* for the first time.

The atmospheric implications of this study are summarized in **Figure 4.1**. The acidity of reactive nitrogen emitted into the atmosphere associated with nitrogen fixation may differ depending on the growth phase of nitrogen-fixing microorganisms, which can further affect the acidity of the atmosphere. This effect includes possible reactions of basic WSON and/or ammonia with sulfuric acid and other acidic species. These reactions may affect gas-to-particle conversion in the atmosphere, leading to an increase in particle number concentrations. Changes in the particle number concentration can affect cloud droplet concentrations produced over the oceanic region and are thus crucial for understanding their climate effects.



Sea-to-air emissions of  $\text{NH}_3$  and WSON:

- [1] **Change acidity of marine aerosol**, which may affect atmospheric chemistry over the ocean
- [2] **Increase aerosol particle number concentrations** by reacting with acidic gas species, and can affect cloud number concentrations

**Figure 4.1** Atmospheric implications of the results obtained in this study.